creative commons
COMMONS DEED

저작자표시-비영리-변경금지 2.0 대한민국

이용자는 아래의 조건을 따르는 경우에 한하여 자유롭게

- 이 저작물을 복제, 배포, 전송, 전시, 공연 및 방송할 수 있습니다.

다음과 같은 조건을 따라야 합니다:

저작자표시. 귀하는 원저작자를 표시하여야 합니다.

비영리. 귀하는 이 저작물을 영리 목적으로 이용할 수 없습니다.

변경금지. 귀하는 이 저작물을 개작, 변형 또는 가공할 수 없습니다.

- 귀하는, 이 저작물의 재이용이나 배포의 경우, 이 저작물에 적용된 이용허락조건을 명확하게 나타내어야 합니다.
- 저작권자로부터 별도의 허가를 받으면 이러한 조건들은 적용되지 않습니다.

저작권법에 따른 이용자의 권리는 위의 내용에 의하여 영향을 받지 않습니다.

이것은 이용허락규약(Legal Code)을 이해하기 쉽게 요약한 것입니다.

Disclaimer

dCollection

공학박사 학위논문

Optimal design and control of silane off-gas recovery process with dividing wall column under periodic disturbances from parallel batch reactors

분리벽형 증류탑을 이용한 병렬식 배치 반응기의 주기적인 외란을 포함하는 실란 배가스 회수 공정의 최적 설계 및 제어

2016년 8월

서울대학교 대학원
화학생물공학부
류 현 철

Optimal design and control of silane off-gas recovery process with dividing wall column under periodic disturbances from parallel batch reactors

지도교수 이종민

이 논문을 공학박사 학위논문으로 제출함

2016년 7월

서울대학교 대학원

화학생물공학부

류 현 철

류 현 철의 박사 학위논문을 인준함

2016년 6월

위 원 장 한 종 훈 (인)

부위원장 이 종 민 (인)

위 원 윤 인 섭 (인)

위 원 이 원 보 (인)

위 원 이 창 준 (인)

Abstract

Optimal design and control of silane off-gas recovery process with dividing wall column under periodic disturbances from parallel batch reactors

Hyuncheol Ryu
School of Chemical and Biological Engineering
The Graduate School
Seoul National University

This thesis has presented a rigorous design and a plant-wide control structure scheme for the effective separation of off-gas from a polysilicon plant with periodic disturbances in the feed. Solar power generation is eco-friendly energy resource, polysilicon is used as a raw material to manufacturing solar cells. In order to obtain the high efficiency of solar cells, it requires ultra-high purity of polysilicon which essentially involves the advanced recovery processes. The target process studied in this thesis produces 10,000 MT polysilicon per year with 28 chemical vapor deposition reactors. The reaction kinetic models were constructed, and their parameters were identified using a genetic algorithm, and that were utilized to design the separation process which separates into hydrogen, hydrogen chloride, and silanes. Though proportional-integral controllers were installed to remove the periodic disturbances, they were not enough to meet the active constraints. A centralized supervisory layer based on model predictive

control to minimize the fluctuation of the recovered concentration, was proposed. Proportional-integral controllers regulates the inventory levels, thereby operating the process stable, and a model based controller showed a good performance rejecting the periodic disturbances. Using a rigorous plant-wide dynamic model, four cases were studied with different control schemes with and without buffer tanks Separated silane off-gas is consist of dichrloro silane, trichloro silane, and silane tetrachloride. Among them, dichloro silane and trichloro silane go into the reactors again. Dividing wall column was designed to achieve the lower energy consumption for the ternary mixture, and control structures were studied. From the novel approach, the energy consumption was decreased up to 37 % compared with classical sequential columns, and the settling time also reduced by proposed research results.

Keywords: polysilicon, silane gas, periodic disturbance, supervisory control, model predictive control, dividing wall column
Student Number: 2012-30254

Contents

List of Figures

List of Tables

Chapter 1

Introduction

Solar photovoltaic (PV) system is currently one of the most attractive forms of renewable energy that uses an abundant and clean energy source such as sun. The amount of carbon dioxide (CO_2) emission from PV system is only about $50\,\mathrm{g}$ of CO_2 per kilowatt-hour (kWh), while traditional power plant generates $975\,\mathrm{g}$ per kWh from coal [1]. In 2013, 37.6 Gigawatts (GW) of PV power plant has been installed and the capacity of cumulative installation was $140\,\mathrm{GW}$ globally [2]. Although the exponential growth of PV system, PV industry has recently undergone because of oversupply and plunging prices. Therefore it is necessary to improve the economic operability and reduce the costs [3].

Polysilicon is base material of PV system, and the silicon feedstock is responsible of about 25-33 % of the silicon based solar module [4, 5]. PV system generates direct current electrical power from semiconductors when they are illuminated by photons. Therefore, a good material with high chemical purity and structural perfection is required to prevent the natural tendency of the conduction-band electrons to return to the valence band. Since silicon is not pure in its natural state and the purity of metallurgical-graded silicon is, at best, 99 % which is insufficient for PV system. It is widely believed that

the required impurity levels for solar-grade silicon are typically less than 1 ppm, or above 99.9999 % (6Ns), which can be achieved by chemical vapor deposition (CVD) of volatile silicon hydride such as trichlorisilane [6]. “the Siemens process” is well known process to produce polysilicon [7]. While the CVD reactor can produce high-purity polysilicon, it requires a long processing time and thus defies mass production. To increase the production rate, the number of CVD reactors that are working simultaneously must be increased.

In the case of polysilicon production, produced polysilicon should be replaced to the seed filaments by operators in batch operation. This causes the reactors to operate in a sequential and periodic manner. And the silane off-gas from the CVD reactors must be further separated and recovered to recycle back to the CVD feed stream in order to increase the material efficiency. Because of the inherent discontinuous and periodic nature of operating the upstream reactors, off-gas recovery process has a strong disturbances periodically such as changes of composition and flow rate.

Although the significant amount of studies exist on the polysilicon manufacturing process, most of them are focused only on thermodynamic analysis [8] and the reactor systems [9, 10]. Not long ago, polysilicon industry achieves the highest profit as the market is oligopolistic by few companies. Silicon purification requires sophisticated design technology and know-how to control the chemical reaction for producing silicon at a competitive price [11]. Most western silicon manufacturers have developed sophisticated know-how in polysilicon industry, but have always been protecting their intellectual property [12]. To the best of our knowledge, there have been no previous studies on the design and control of the polysilicon off-gas

recovery process for this reason.

Many control studies, which are based on first-principles plant models, focus on the operability and controllability of a specific portion of the plant or only several units without considering real-plant scale and plant-model mismatch. Even if in the area of plant-wide control, most works [13] have based on steady-state model which is not adequate in polysilicon process. The recovery process should be analyzed together not only CVD reactors but also separation units, because the flow rate and composition of the off-gases from reactors periodically change and act as disturbances. Oftentimes, the recovery units are oversized, relative to the required capacity, by the need to consider the upper and lower bounds of the flow rate and composition disturbances at the process design stage. However, considering the interplay between control and design can address this issue; a plant-wide control scheme with rigorous dynamic models in the process design step can help yield a more optimal design.

In this thesis, silane off-gas recovery process is designed on the basis of industrial scale, 10,000 MT of polysilicon per year, with 28 CVD reactors by the proposed modeling scheme with periodic disturbances. In order to obtain a rigorous dynamic model, CVD reaction kinetic models were constructed, and their parameters were identified using input-output empirical data. Due to the inherent absence of a steady state, one particular reference point (OP-RP) was adapted in the beginning of the process design step. The OP-RP refers to a state of the off-gas that averaged the values obtained from the parallel batch reactors. Using a customized reactor model, the OP-RP process that is actually cyclic steady state was designed and optimized for the entire process.

The off-gas recovery process and the periodic sequential operation procedure of CVD reactors was implemented in Aspen Dynamics^{TM}. In order to minimize the fluctuation of the recovered concentration, the different control schemes compared between fully decentralized proportional-integral-derivative (PID) controllers and model predictive control (MPC) based supervisory control over PID controllers with and without buffer tanks.

The byproduct stream leaving the CVD reactor contain Hydrogen gas (H_2), Hydrogen Chloride (HCl) and silane off-gases such as SiH_2Cl_2 (dichlorosilane, DCS), $SiHCl_3$ (trichlorosilane, TCS), and $SiCl_4$ (silicon tetrachloride, STC). Among them, silane off-gas is relatively heavier than H_2 and HCl, and they are lastly separated for each one. The relative volatilities of DCS, TCS and STC are 1, 1.9 and 3.4. For the separation of multicomponent mixtures, most often a sequence of distillation columns is applied. When separating three components such as silane off-gas, at least two columns are necessary. However, there has been reported that a dividing wall column (DWC) can lead to improve energy efficiency up to 30 % compared with sequential columns [14]. For the separation of silane-off gas, optimization for DWC design was performed and controllers were tested to meet the product specifications.

Chapter 2

Overview of process and methodology

Polysilicon process is represented by purification which is convert metallurgical-grade silicon to ultrahigh purity of silicon (solar-grade silicon). The entire process is described in Fig. 1. Only silicon is input and output at the same time. Small amount of make-up such as H_2, HCl, STC is necessary to keep the operation in stable process. Ultrahigh purity is achieved first by preparing a volatile silicon hydride typically, TCS which is prepared by the hydrochlorination of metallurgical-grade silicon in a fluidized bed reactor and its purification, which generally requires fractional distillation. High purity of TCS can affect the purity of polysilicon, generally lots of energy is consumed in the TCS purification process. High purity TCS is diluted with high purity hydrogen gas (H_2) and then introduced into the CVD reactors. In the CVD reactor, decomposition of the hydrides to hyperpure elemental silicon is occurred by reductive pyrolysis or chemical vapor decomposition. The gas is decomposed onto the surface of the heated silicon seed rods, and the by-product streams leaving the reactor contain H_2, HCl, and silanes such as DCS, TCS, and STC. Because there is no large-scale industrial application for STC, it has to be collected and converted to TCS. Therefore, the off-gas from the CVD reactors needs to be further separated and recovered to recycle

back to the CVD feed. The entire process is fully closed and continuous except for CVD reactors. In this thesis, blue blocks are the scope of design and control because that dominate polysilicon process.

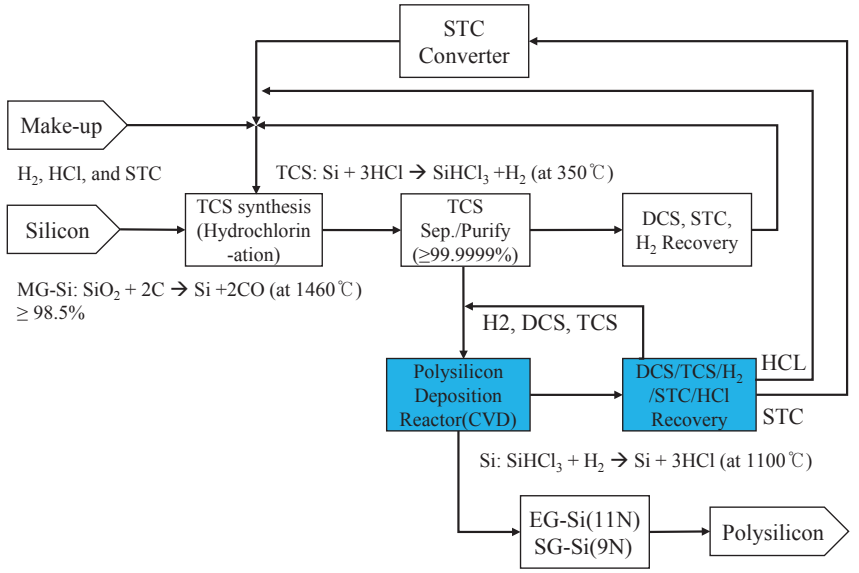

Figure 1: Block flow diagram of polysilicon process; EG-Si: electric-grace silicon for semiconductor, SG-Si: solar-grade silicon for solar cell

CVD reactors run in batch mode, and each reactor has a repetitive operation procedure. One cycle of the operation procedure is composed of three steps: pretreatment, deposition and maintenance. In the pretreatment step, seed filaments are set into the CVD, and then the reactor is stabilized by a gas purge procedure. During the deposition step, silicon rods are grown simultaneously with off-gases, and the produced polysilicon is then recovered in the maintenance step. The off-gas lines from each reactor merge into a single pipeline. As a result, periodic fluctuations in the feed flow rate and composition of the recovery process are inherent as shown in Fig. 2. The subsequent

separation processes to recover H2, HCl and silanes run in continuous mode. Whereas most of the plant-wide control systems use a steady state model, new process design and control schemes are needed to handle the fluctuations for a separation process integrated with parallel batch reactors.

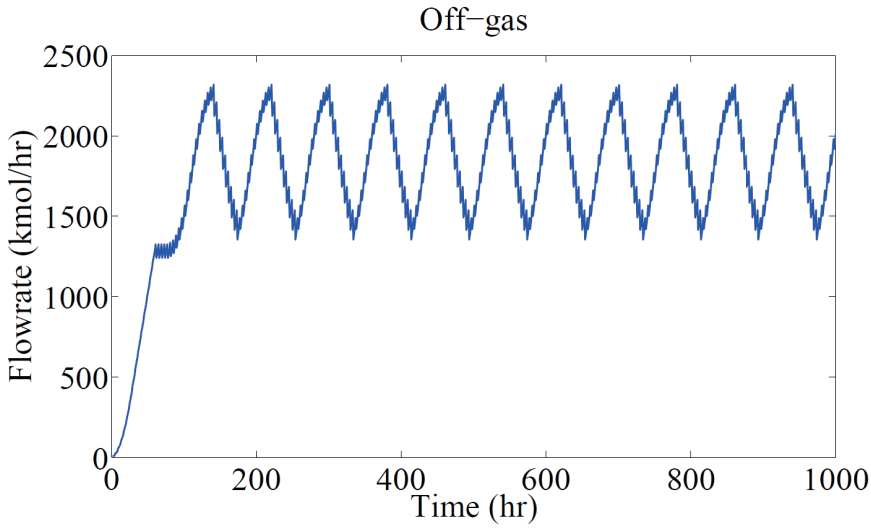

Figure 2: Periodic disturbance from parallel batch reactor

In cyclic steady state operation, it is difficult to separate process design and control. Steady state-based set point calculation tends to keep the regulatory control around a fixed operating point or within a narrow operation range, which is obtained by optimizing the economic performance under a given operating objective. However, in the cyclic steady state, batch processes bring about strong disturbances to the continuous processes that may cause a violation of the operating constraints. In this thesis, process design and control are interweaved in that an optimal process design cannot be found be-

fore dynamic simulations are performed with an appropriate control structure. Sakizlis et al. [15] discuss recent advances toward the integration of process design and control. Other existing methods [16, 17] also show the advantages of simultaneous design and control with a similar motivation with this thesis. Fig. 3 shows a proposed approach that considers process design and control simultaneously. It consists of two steps: a top-down approach is adapted to process design and optimization, and a bottom-up approach is applied to process control and operation. From the control study, process design should be revisited to incorporate a developed control scheme. This differs from the procedure proposed by Skogestad [18], which considers only the control structure. First, from the top-down approach, the process target is set to satisfy the production plan. Once the amount of polysilicon is specified, a customized batch reactor model is necessary to calculate the number of reactors, given the constraints of the production rate and reactor maintenance time. Then, the OP-RP model is constructed using the developed dynamic batch reactor model. Though the recovery processes are running in continuous mode, they do not have a steady state with the batch reactors integrated. Using the resulting OP-RP model, the operating point can be identified by optimizing the economic performance. Second, in the bottom-up approach, the OP-RP model is further developed into a dynamic model to determine the control scheme. Given the equipment sizing in the first stage, the pairing of manipulated inputs and controlled outputs is performed. The parameters of the PID controller are also tuned. Then, dynamic simulation is performed to confirm the active constraints and product target. If a model does not satisfy the active constraints because of the periodic disturbance, a supervisory controller can be used to adjust

the set-points of the regulatory controllers. Especially for the polysilicon process, which requires an ultra-pure product, critical units such as distillation columns are very sensitive to changes in the manipulated variable. Therefore, controlling only the distillation columns cannot reject the periodic disturbance, so a proper plant-wide control is required. Finally, the process design parameters are updated based on the control scheme. Hence, the suggested approach iterates between process design and dynamic simulation under a supervisory control scheme to handle periodic disturbances from a set of parallel batch reactors affecting the operation of continuous separation processes.

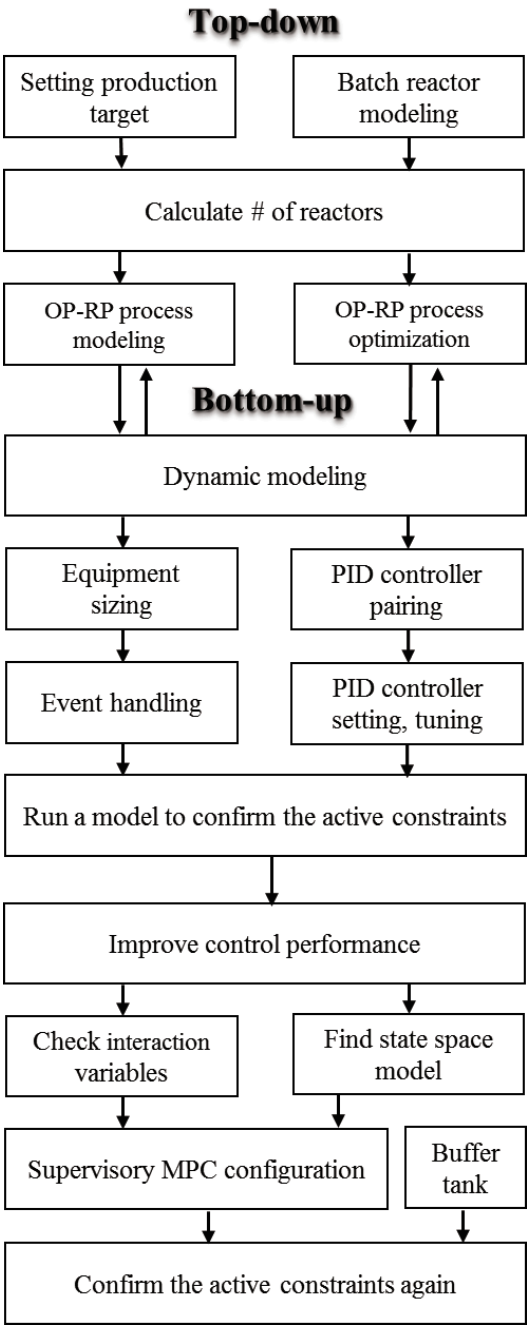

Figure 3: Modeling scheme with periodic disturbances

Chapter 3

One particular reference point based modeling of off-gas recovery process

3.1 Introduction

The silane gases consist of dichlorosilane (DCS, SiH_2Cl_2), trichlorosilane (TCS, $SiHCl_3$) and silicon tetrachloride (STC, $SiCl_4$). Metallurgical silicon is a raw material for producing TCS, which is subsequently used to produce polysilicon. This process requires a high percentage of the H2, HCl, and silanes to be recycled during production, thereby reducing the waste output and lowering the make-up. In this chapter, CVD reactor and silane off-gas recovery process was investigated for the purposed of developing modeling scheme with periodic disturbances [19]. CVD reactors are operated sequentially, so it is difficult to calculate nominal operating parameters. To design the silanes' off-gas recovery process, OP-RP process which refers to a state of the off-gas that averaged the values obtained from the parallel batch reactors were first used. And also with the OP-RP process model, optimization was performed to maximize the economics. At the first step, kinetics of CVD reactor was constructed, then the parameters of kinetics were identified. From the reactor model, the number of required CVD reactors can be calculated. The annual pro-

duction target was set to 10,000 MT per year. From one cycle of CVD reactor operation, 3,600 kilograms of polysilicon were produced, and one cycle took 80 hours. To meet the production target, more than 28 CVD reactors would be necessary. One additional reactor was set to hedge against emergency situations such as the unplanned shut down of reactors. All of the off-gas from the reactors was combined into a single pipe line, connected to the recovery section. The recovery section is a continuous process, and a rigorous dynamic model is required to test the controller performance on the plant-wide scale. In this thesis, it is assumed that all the recovery units have total condensers. The molecular weight of H_2 is small, however its molar flow rate is greater than sum of rest off-gas. Therefore, it is necessary to separate the H_2 first for the reduction of equipment size. And also, to separate the H_2, the off-gas needs to be cooled a low temperature and high pressure using a compressor and heat exchangers, and it causes the incresed operation cost. Hence, the direct sequence was applied for the recovery process, the H_2 was first recovered by a packing column, and then HCl was recovered by a distillation column. Finally, STC was separated from DCS and TCS.

3.2 Identification of CVD reactor kinetics

Chemical vapor decomposition (CVD) reactors are widely used for solid material production from gaseous reactants. There are various types of CVD processes, but for silicon-based photovoltaic technology, the chemical route through CVD, which is known as “the Siemens process”, presently dominates the production of polysilicon. The Siemens process is more stable than a fluidized bed reactor. The

fluidized bed chemical vapor deposition (FBCVD) method [10] is a most promising alternative to the Siemens process, but the homogeneous reaction of silanes in FBCVD results in the unwanted formation of fines, which will affect the product quality and output [20]. The Siemens process also has some limitations of batch operation. Each reactor requires a maintenance period after one batch cycle, while the number of operated reactors is specified to meet the production target. Once a CVD reactor is turned on, it runs for sixty hours, and then it takes twenty hours for maintenance. In the maintenance period, the produced polysilicon is recovered and the CVD reactor is reset to the initial condition. After the maintenance is completed, the CVD reactor operates again. Because a single CVD reactor has a capacity limit, a number of reactors are operated in parallel. There have been many studies to identify the kinetics [21, 22] and thermodynamics of manufacturing polysilicon [8]. Because the reaction mechanism of the chemical vapor deposition of silicon is complex with a number of radicals formed, it is difficult to obtain all of the kinetic parameters [23]. However, five reactions [22] related to the inputs and outputs are sufficient to describe the CVD reactor in this thssis. The reactor system has three reactants (H_2, DCS, TCS) in the inlet, two intermediates ($SiCl_2$, SiH_2Cl_2), and six outputs (H_2, DCS, TCS, STC, Si, HCl). The main reaction pathway is from TCS to polysilicon, as shown in Fig. 4. Some gases are thermally decomposed in the bulk space, and other gases are deposited on the silicon rod surface. The deposited gases are transformed to adatoms, which are converted to polysilicon or would etch silicon.

$$SiHCl_3 \leftrightarrow SiCl_2 + HCl \tag{3.1}$$

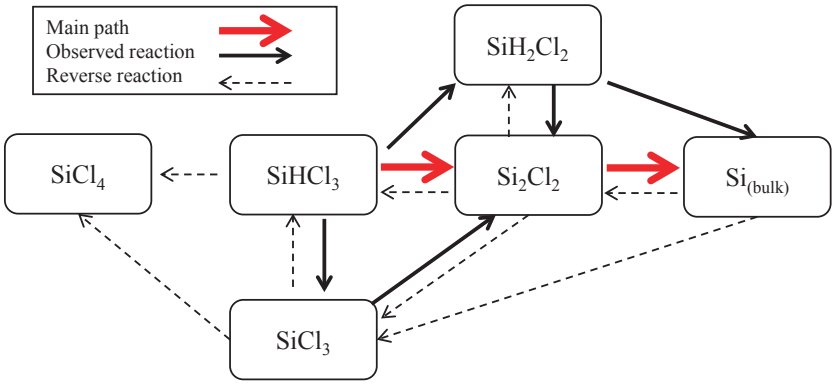

Figure 4: Key reactions for production of polysilicon

$$SiH_2Cl_2 \leftrightarrow SiCl_2 + H_2 \tag{3.2}$$

$$SiH_2Cl_2 + HCl \leftrightarrow SiHCl_3 + H_2 \tag{3.3}$$

$$SiHCl_3 + HCl \leftrightarrow SiCl_4 + H_2 \tag{3.4}$$

$$SiCl_2 + H_2 \leftrightarrow Si_{bulk} + HCl \tag{3.5}$$

Eqs. (3.1) and (3.2) represent the thermal decomposition of the raw material (DCS, TCS), and Eqs. (3.3) and (3.4) show that HCl participates in low-temperature reactions. Eq. (3.5) represents an ion radical reaction to produce polysilicon. All of the kinetic parameters of the empirical model were found by using Arrhenius equation. The product composition depends on the temperature of the rod surface and inlet gas composition. Because the production rate of polysilicon is dependent on the rod temperature, using the input-output data of CVD reactor with varying temperatures, reaction parameters such as pre-exponential factor, activation energy and the order of reaction

with respect to inlet gas composition were identified using nonlinear least squares. In MATLAB environment, a genetic algorithm [24] was used to solve the nonlinear optimization problem. The genetic algorithm is a stochastic, and global search algorithm that is widely used in a number of fields due to its advantage over other deterministic optimization methods, especially for the nonlinear parameter estimation [25, 26]. Reference data were used each for input, output composition and temperature during the one cycle of CVD, then minimized the differences between sampled output data and their model predictions. The resulting parameters show good agreement with the reference data. There are some differences at the end of reaction, because the exact surface temperature of silicon rod can not be measured in practice. However, these are not important in this thesis, on the other hand, it can be simply represented by piecewise linear regression. Finally, this reactor model in Eqs. (3.6) - (3.12) was integrated into an Aspen Dynamics^{TM} simulator of the entire process using Aspen Custom Modeler^{TM} (ACM).

$$\frac{[TCS]_{out}}{dt} = 26.445exp\left(\frac{-7887.8}{T}\right)[H_2]_{in}^{1.137} \tag{3.6}$$

$$\begin{aligned}\frac{[STC]_{out}}{dt} = 1.929exp\left(\frac{1117}{T}\right)[TCS]_{in}^{0.876} \\ -4.268exp\left(\frac{-95.271}{T}\right)[TCS]_{in}^{0.866}\end{aligned} \tag{3.7}$$

$$\frac{[DCS]_{out}}{dt} = 6.611exp\left(\frac{8371}{T}\right)[TCS]_{in}^{-0.089}[H_2]_{in}^{1.196} \tag{3.8}$$

$$\frac{[H_2]_{out}}{dt} = 4.304[TCS]_{in}^{0.948} - 0.208\,[DCS]_{in}^{0.95} \tag{3.9}$$

$$\frac{[HCl]_{out}}{dt} = 0.149[TCS]_{in}^{0.781} - 0.206\,[TCS]_{in}^{1.28}[H_2]_{in}^{-0.605} \quad (3.10)$$

$$\frac{[SiCl_2]_{out}}{dt} = 0.149[TCS]_{in}^{0.126} - 0.208\,[DCS]_{in}^{0.126} \quad (3.11)$$

$$\frac{[Si_{bulk}]_{out}}{dt} = 0.186exp\left(\frac{12101}{T}\right)[DCS]_{in}^{3.584}[TCS]_{in}^{-2.3}[H_2]_{in}^{-0.159} \quad (3.12)$$

3.3 OP-RP process simulation

The separation sequence is the order of lower boiling point. Fig. 5 shows the flowsheet for the off-gas recovery process. Off-gas is generated from CVD reactors and they contain H_2, HCl, and silanes (TCS, DCS, STC). The process consists of four stages. In this thesis, off-gas is cooled by two coolers and one heat exchanger was installed to enhance the heat recovery in the first stage. Then, flash drum (FLASH) and compressor (Compr) partially condense the off-gas. In the second stage, the compressed gas gets together with recycled HCl stream, then it is separated into a high-purity H_2 and HCl rich liquid in the packed desorption column (PDC). In the third stage, liquid streams from FLASH and PDC are sent to the HCl separation column (HCl-col). HCl-col is designed to recover a high-purity HCl at the top and returns the silanes to the STC separation column (STC-col) at the bottom. In the fourth stage, stream from the bottom of HCl-col is split into two streams. One is fed into the STC separation column (STC-col) and the other is recycled to PDC. In the STC-col, DCS and TCS are recovered from STC and reused in CVD reactor. The OP-RP process was simulated in Aspen Plus^{TM} environment using NRTL (Non Random Two Liquid) equation of state.

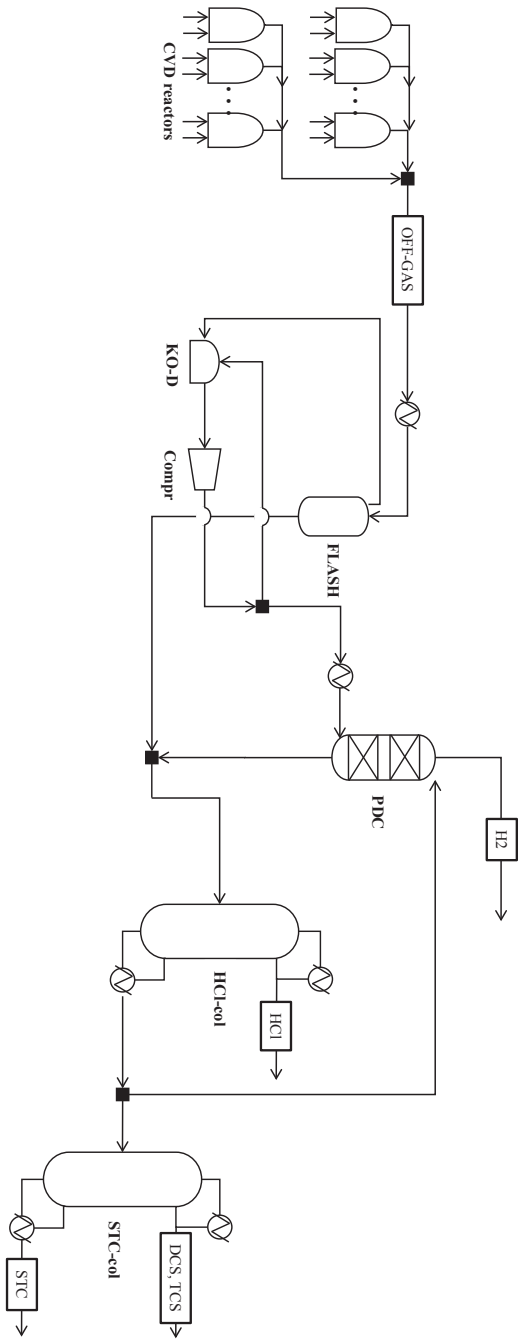

Figure 5: Flowsheet of off-gas recovery process

The OP-RP process were designed to satisfy the product specifications. There are three columns to recover H_2, HCl, and STC. The H_2 separation column has a target of 99.8 mol %, and the HCl separation column has a target of 99.9 mol % as shown in Table1. The STC column separates STC to almost 100 mol %. All the columns were optimized to minimize the energy consumption through a total stage and feed tray position analysis. As a result, the feed stage of the HCl column was 19 out of the total 27 stages, and the STC column feed stage was 91 of 167 stages.

Table 1: Design of the columns for the off-gas recovery

Unit	Separation target (mol%)	Design sepc (purity)	Vary
PDC (H_2)	99.8	-	-
HCl-col (HCl)	99.9	Top HCl: 0.999	Molar distillate rate
STC-col (STC)	100	Top STC: 0.001	Molar reflux ratio

The H_2 column was a packed desorption column, and the last two columns were distillation columns with a condenser and reboiler. Conventionally, tray temperatures are widely used for the inferential control of compositions. Therefore, the last two column units (HCl-col, STC-col) should be analyzed for the control structure. The reflux ratio (U1) and reboiler duty (U2) were selected to be the manipulated variables for the columns. Then, 0.1 % of the step changes were introduced in the manipulated variables, and their output responses are shown in Fig. 6. Fig. 6 shows four profiles of each column. The first graphs [(a) and (e)] represent temperature profile in the column.

The second graphs [(b) and (f)] show temperature slope from tray to tray. This is a slope criterion to select the tray where there is a large change in temperature from tray to tray. Maintaining a tray temperature at this location will effectively hold the composition profile in the column. The third [(c) and (g)] and fourth graphs [(d) and (h)] give information on the change of MVs. The third graphs show the sensitivity criterion to find the tray with the largest change in temperature given a change in the manipulated variable. Lastly, the fourth graphs represent left singular values to select the tray with the largest magnitudes of U. In Fig. 6, Sensitivity and scaled singular value decomposition (SVD) analyses [27, 28] show that the temperatures of tray 3 for the HCl separation and tray 15 for the STC separation are controlled by the reboiler duty. Fig. 6 (b) represents the temperature difference from tray to tray in the HCl separation column. It shows a sudden change near a tray 4 by up to 60 °C. This means that it is not easy to control the tray temperature in the presence of disturbances. When the set-point of the tray temperature is changed, the PI controller may make the process unstable. Hence, the reflux to feed ratio was additionally regulated via feedforward control to reduce the effect of feed flowrate disturbances.

3.4 Optimization with OP-RP process

With the OP-RP process model, optimization was performed to maximize the economics. The economics is strongly affected by the recycle flowrate. When the molar purity of HCl was kept at 0.999 in the HCl-col overhead, variations of the recycle flow rate at SPLIT the reboiler heat duty of the HCl column, and the impurity of the H_2

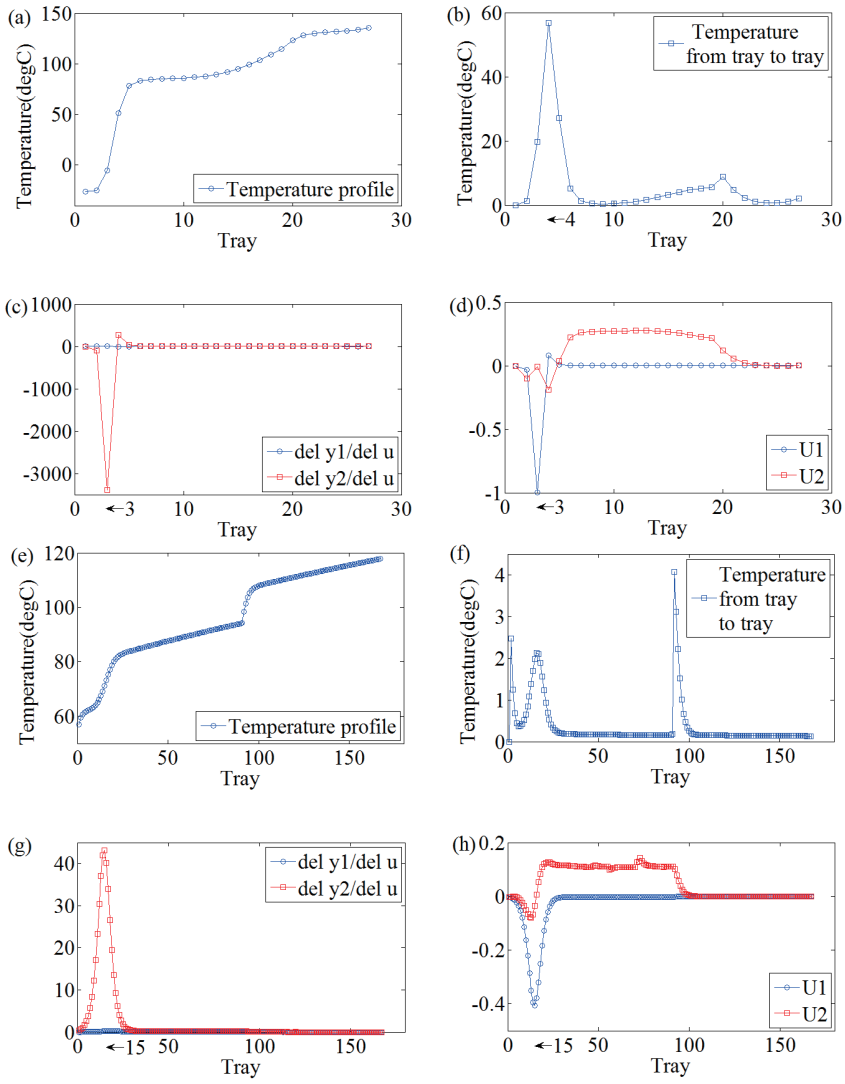

Figure 6: Column profiles of HCl [(a)-(d)] and STC [(e)-(h)] separation columns; (a) and (e) temperature profile, (b) and (f) temperature difference from tray to tray, (c) and (g) sensitivity analysis, (d) and (h) left singular vector

flow were analyzed, while STC-col does not affected by the change of recycle flowrate; the results are shown in Fig. 7. The reboiler duty continuously decreased as the recycle flow rate decreased to meet the design specification of 0.999 in the HCL-col overhead. However, impurities in the H_2 stream suddenly increased below a recycle flowrate of 680 kmol/hr because there is no manipulated variable in PDC. At the results, in order to reduce the operating cost, the recycle flowrate had a limitation of H_2 stream and it was set to 680 kmol/hr in the process design stage. The final OP-RP model is shown in Fig. 8.

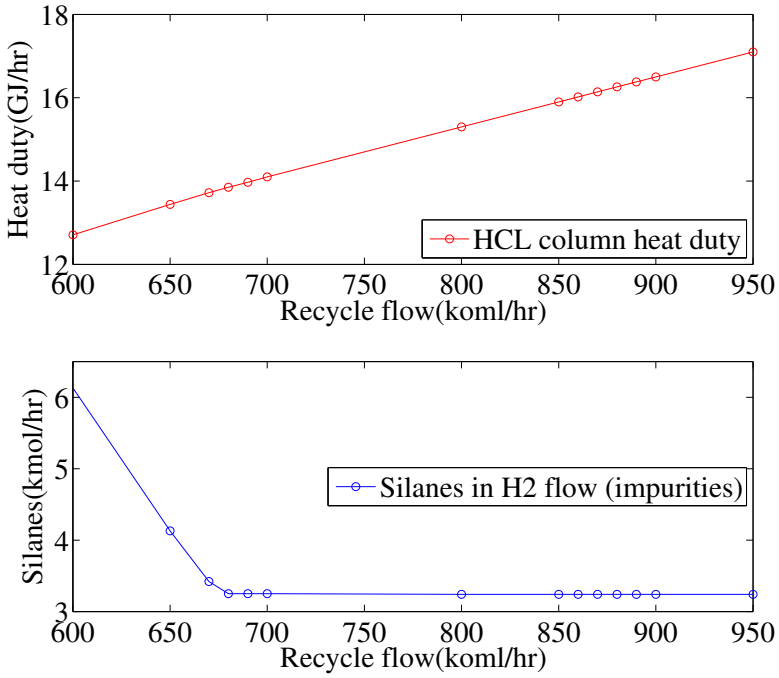

Figure 7: OP-RP process optimization

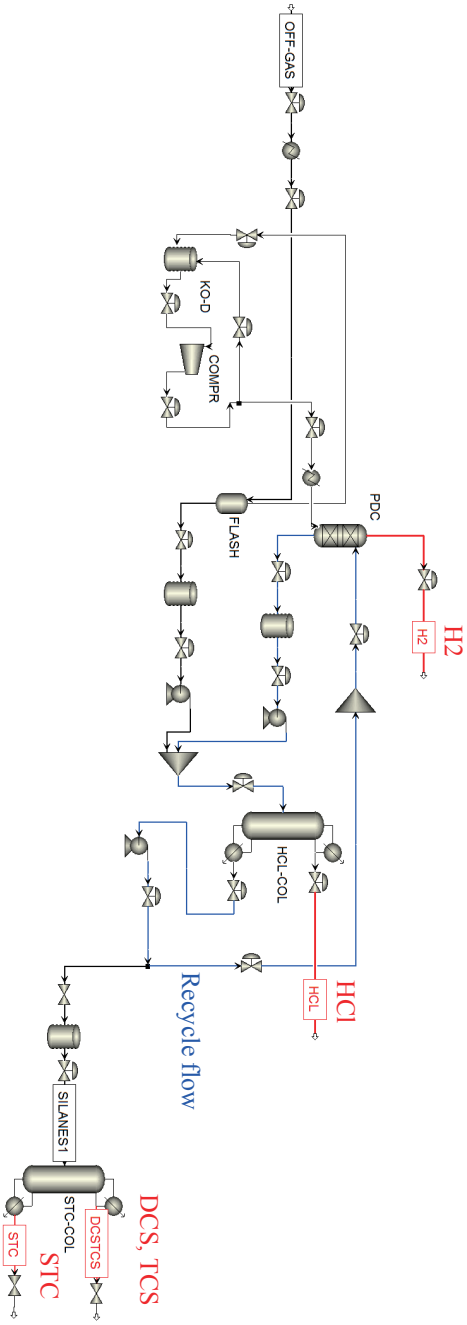

Figure 8: OP-RP process simulation environment

3.5 Conclusion

In this chapter, the silane off-gas recovery process is designed for the separation of H_2, HCl, and silanes for developing a top-down part of proposed modeling scheme with periodic disturbances. The recovered purity of H_2 is 99.8 mol %, HCl is 99.9 mol %, and STC is about 100 mol %. These values can be reused to polysilicon manufacturing process. The kinetics of conventional CVD reactor was constructed, then its parameters were identified. From the CVD reactor model, industrial scale of 10, 000 MT of polysilicon per year was investigated and optimized to reduce the operating cost. Less recycle flowrate is better in utility cost, however desorption column for H_2 recovery can be violate the product target, recycle flowrate was optimized. The developed OP-RP model will be able to convert dynamic model and be useful to design the process with periodic disturbances from parallel batch reactors.

Chapter 4

Dynamic modeling and control studies of silane off-gas recovery process

4.1 Introduction

In this chapter, various control schemes were performed to handle the periodic disturbances with developed OP-RP process. Most works [13] in the area of plant-wide control have focused on controller design using a steady state model. Traditionally, control structures are designed based on heuristic methods [29, 30] that do not use process knowledge in a systematic manner. Recently, a systematic model-based approach for control structure design was proposed [31] using a two-stage method, starting with a top-down analysis and ending with a bottom-up design. In the first stage, a top-down approach is taken to generate a list of manipulated, controlled, and disturbance variables, considering a scalar operation objective and other process constraints. In the second stage, a bottom-up approach is used to design a control system given the results from the previous stage. Though this approach has been reported in a number of previous studies [32, 33, 18, 34], it has been rarely applied to processes that involve batch reactors due to the inherent absence of a steady state. Model predictive control (MPC) is the most popular model-based control

scheme and possesses the flexibility to handle constrained multivariable and non-square systems with time delays while permitting the use of several modeling forms. To handle the periodicity of processes within the model-based control framework, Lee et al [35] developed repetitive model predictive control (RMPC), which borrows the idea of periodic error rejection from repetitive control (RC). Subsequently, many studies [36, 37, 38, 39] incorporated the ideas of RC and iterative learning control (ILC) into MPC frameworks to address periodic disturbances. These methods, however, impose a great computational burden and are thus not realistic for practical applications such as the polysilicon process because of the model complexity and material recycle loop, though period time can be varied by scheduling. Hence, a simple control scheme is necessary to handle the periodic disturbances. In this thesis, using a rigorous plant-wide dynamic model, four cases were studied with different control schemes with and without buffer tanks.

4.2 Dynamic modeling of OP-RP process

There are two different approaches to dynamic simulation within commercial dynamic simulators. One is the pressure-driven mode, which is preferred when the pressure of the system is important as in the gas phase. The other is the flow-driven mode, which is suitable for liquid phase systems or systems with good pressure and flow control. This study adopts the flow-driven mode for rigorous dynamic simulation. An empirical model of the CVD reactor in Eqs. (3.6) - (3.12) of chapter 3 was developed in Aspen Custom Modeler^{TM}. The OP-RP process model of the entire process developed in Aspen Plus^{TM} was

also imported into Aspen DynamicsTM. The converting procedure from steady state simulation to dynamic one using Aspen products as follows: Aspen Dynamics^{TM} uses the steady-state information generated in Aspen Plus^{TM}. Therefore, before converting the OP-RP process model to an initial dynamic one, the equipment sizes must be specified for the major equipment, such as the buffer tank, column, reflux, and condenser drum. The packing and tray-sizing tool of Aspen Plus^{TM} can conveniently calculate the column diameters. Pumps were installed to compensate for the pressure drops from valves and equipment. After a pressure-check was performed for the whole OP-RP process flowsheet, then push the button "Sent to Aspen Plus^{TM} Dynamics" to create the file of Aspen Dynamics^{TM} model. More details about this procedure can be found elsewhere [40]. A typical plant has many controllers for flow, level, pressure, temperature, and other parameters. The controllers must be specified, e.g., PI, PID, DMC, MPC, and nonlinear, and tuned. An important goal of dynamic simulation is to develop an effective base-level regulatory control structure. In this thesis, linear PI controllers were first installed in a decentralized (single-input-single-output; SISO) environment to stabilize the plant. Controller tuning was based on sequentially closing and tuning one loop at a time, starting with the fastest loop. Using the Aspen Dynamics^{TM} open loop test, a first-order plus time delay model was obtained. Based on the model parameters, SISO-IMC tuning rules [41] for the PI-controller were used as follows:

$$K_c = \frac{\tau_p + \frac{\theta}{2}}{K_p \lambda}, \quad \tau_I = \tau_p + \frac{\theta}{2} \tag{4.1}$$

where K_c is the controller gain and τ_I is the integral time con-

stant. K_p, τ_p and θ are the process gain, time constant and effective time delay, respectively. λ is a filter parameter and it must be greater than 0.2 times the calculated process time constant. For a PI controller, λ must be greater than 1.7 times the dead time. A smaller value of λ gives a faster response. In this thesis, the minimum recommended value of the tuning parameter [42], $\lambda = \max [0.2\tau_p; 1.7\theta]$ was used, to provide smooth control with acceptable regulation performance. Flow controllers were used the values of 0.5 and 0.3 min for the controller gain and integral time constant. And level controllers were used the value of 2 for gain, and 9999 min for integral time constant. After all the regulatory controllers were implemented and tuned using PI controllers, the initial states could be calculated in Aspen Dynamics^{TM}. The CVD reactors were sequentially turned on at 4-hour intervals, and each reactor had 80 hours for cyclic batch operation as shown in Fig. 9. This operation could be simulated using the task function in Aspen Dynamics^{TM}. All of the 28 reactors were periodically operating in parallel then, cyclic-steady state was reached after 140 hours. This thesis assumed that to control the cyclic-steady state process the following active constraints should be satisfied.

1) Molar purity of recovered $H_2 \geq 0.997$
2) Molar purity of recovered HCl ≥ 0.9985
3) Molar purity of recovered STC ≥ 0.999

The silanes' off-gas recovery process needs a high degree of purity and consumes energy intensively. The PI controller has a good performance for making the process stable, but basically, it cannot respect the constraints. If the active constraints are not satisfied with

only the PI controller because of strong disturbances from the batch reactors, then it is necessary to compensate the control structure or retrofit the process design. In this chapter, dynamic simulations of 380 hours were tested for the supervisory as well as regulatory layers. In addition, the buffer tank is tested for whether it can reduce the effect of periodic disturbances to the process design perspective.

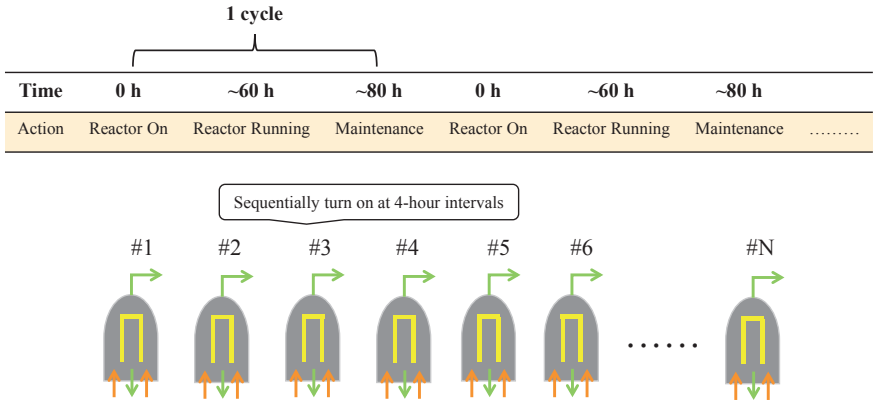

Figure 9: Periodic operation of CVD reactors

4.3 Conventional control schemes for silane off-gas recovery

4.3.1 Case1. PID with feed-forward control

In this case, conventional control structure such as decentralized PI controllers without a buffer tank was tested in order to reject the periodic disturbances. The set-points of controllers were determined from the OP-RP process simulation. The key control points are pressure of PDC, purity of HCl, and purity of STC. Conventionally, in-

ferential control is preferred, therefore tray temperatures were used for the inferential control of compositions, and which are already determined in chapter 3. The temperature of tray 3 for the HCl separation and tray 15 for the STC separation are controlled by the each of reboiler duty. The major disturbances are the feed flowrate and composition from the CVD reactors. In the HCl distillation column, feed-forward controller was used to reject the flow disturbances, the reflux rate was set to 14 % of the feed flowrate at the OP-RP process condition. In the STC distillation column, recovered DCS and TCS require high purity in order to be directly re-used in the CVD reactors. Hence, the reflux flow rate was set to be 1.37 times as high as the feed flowrate of the column. After all of the PI controllers were tuned, dynamic simulation was performed for 380 hours. The process flowsheet and the results are shown in Fig. 10 and Fig. 11.

As Fig. 10 shows, the purity of the recovered H2 (a) and HCl (b) did not satisfy the constraints (red lines) because of the fluctuations in the mixed effluent from the CVD reactors. However, all of STC (c) was separated from DCS and TCS because of high reflux rate. Periodic disturbances influence all the units of the process, and the SISO controllers could not reject these disturbances because the process had some time delays and they also did not consider interactions among the manipulated variables. When the flowrate of effluent (d) was increasing, the purity of recovered H2 was decreased and then HCl purity was increased subsequently. PI controllers tried to keep the set-points such as the temperature controller (TC) of HCl column ((e), -4.1 °C), but periodic disturbances continuously affected the controllers before they rejected the disturbances. The reboiler duty of HCl separation column (f) was also fluctuated following the

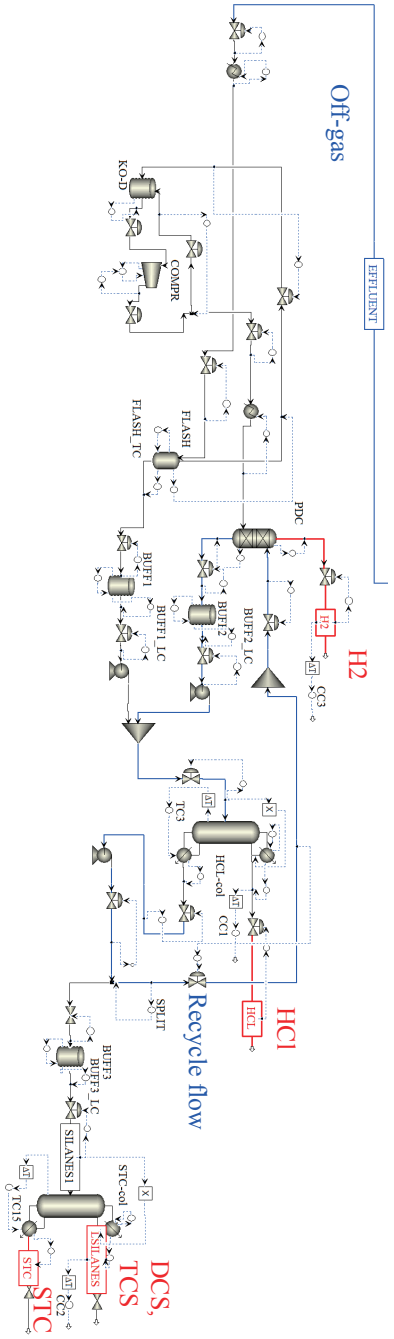

Figure 10: Process flowsheet for off-gas recovery in polysilicon process

flowrate of effluent. In this situation, there are two options: retrofit the process design or implement a supervisory control scheme. The former is simply implemented by using a buffer tank which can reduce the flowrate and composition disturbances. By fixing the outlet flowrate of the buffer tank, the feed flowrates to HCl and STC distillation columns can be regulated. The latter means that the set-points of PI controllers would be changed by MPC as model based controller.

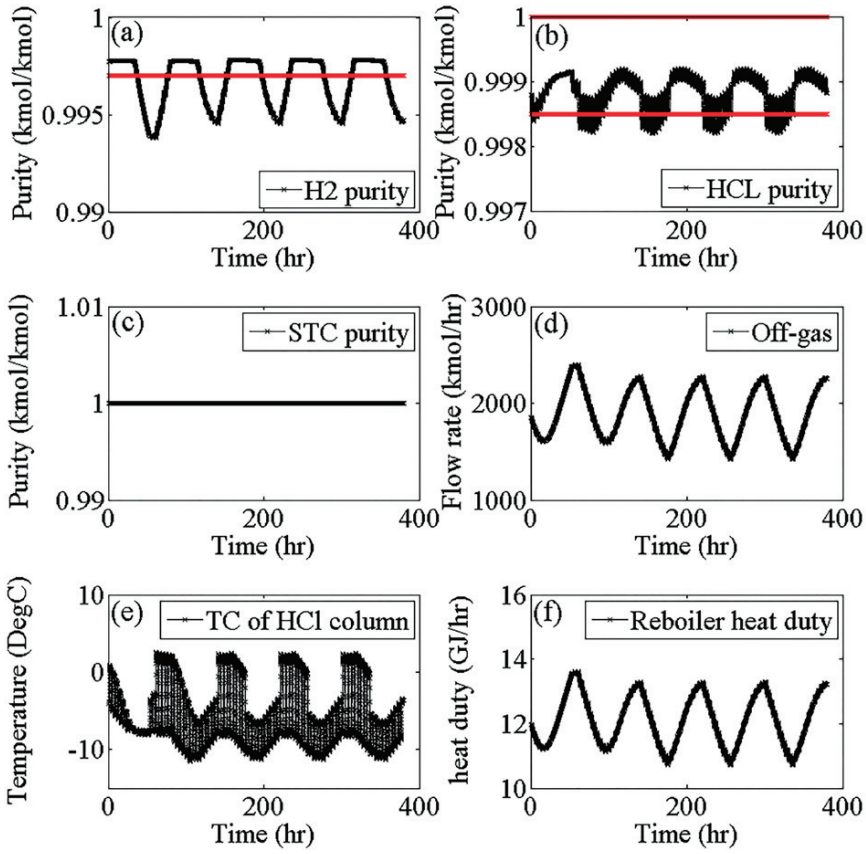

Figure 11: Performance of regulatory controllers

4.3.2 Case2. PID with feed-forward control + buffer tank

In order to reduce the flowrate disturbances, it is possible to install a buffer tank before the column units only for HCl and STC. Because the packing column to recover H_2 treats the gas phase of the feed stream, a buffer tank cannot be used. The capacity of the buffer tank was sized to handle the flowrate fluctuation. The size of the HCl buffer tank was 9 m $\times$ 20 m [diameter $\times$ length], 7 m $\times$ 15 m [diameter $\times$ length] for the recycle buffer tank and 5 m $\times$ 10 m [diameter $\times$ length] for the STC buffer tank. The process flowsheet is shown in Fig. 12.

In Fig. 13, (a) shows H_2 purity is still violated the constraints, but the purity of recovered HCl (b) satisfies the active constraints because a buffer tank reject the flowrate disturbance. TC (temperature controller) of HCl separation column (e) is well regulated the set-point despite the composition disturbance. Moreover, the variation of the reboiler duty (f) in the HCl column was reduced. It is advantageous to specify a reboiler size with a small variation. If the maximum duty is far from the normal operating condition, then the reboiler size must be increased. Compared with the no buffer tank case (Sec. 4. 3. 1), the maximum heat duty decreased from 14 to 12 GJ/hr, almost 15 % of the total capacity. Additionally, this will allow the heat exchangers to be of smaller size in the recycle lines. Using the buffer tank, the process could be operated more stably and the plant oscillation was reduced compared with the case of no buffer tank. Even with the buffer tank, however, the recovered H_2 purity did not meet the specification because the vapor stream cannot use a buffer tank.

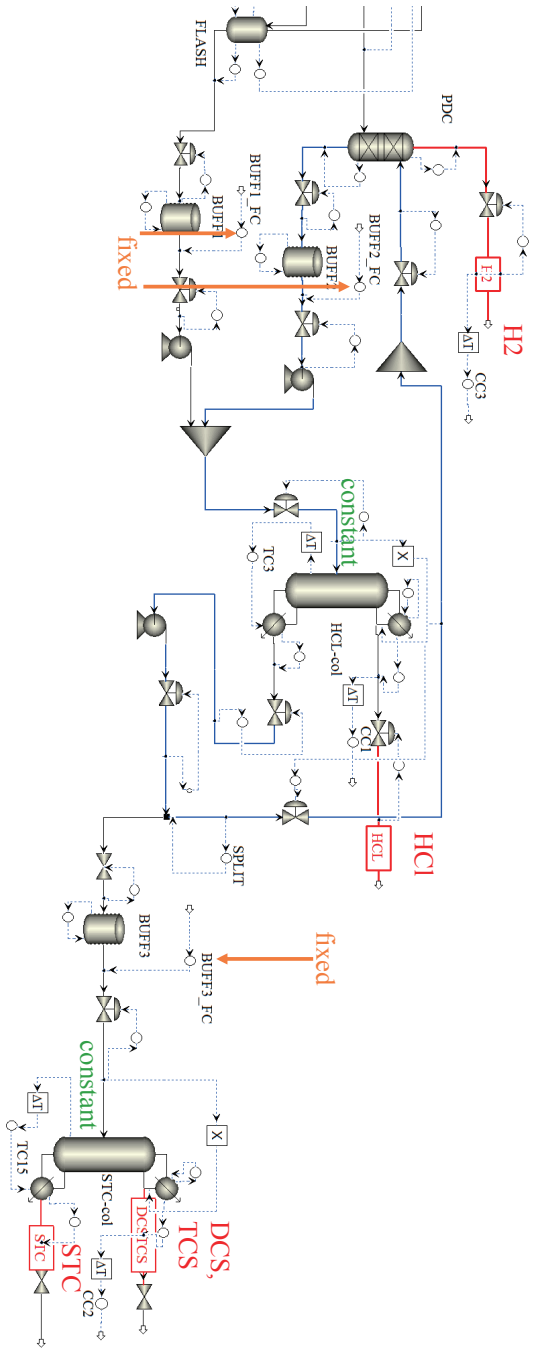

Figure 12: Process flowsheet with buffer tanks

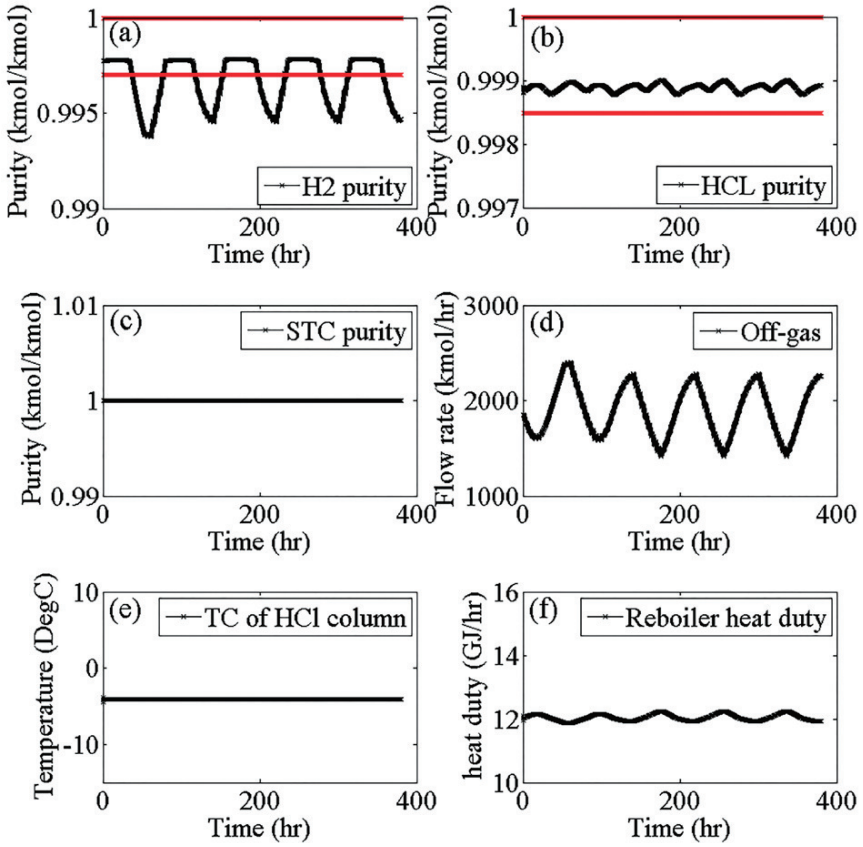

Figure 13: Performance of regulatory controllers with buffer tanks

4.4 Proposed control scheme

4.4.1 Supervisory control based on MPC

The purpose of the supervisory control layer is to keep the primary controlled outputs at their optimal set-points, using as degrees of freedom the set-points in the regulatory layer and any unused manipulated inputs [31]. Although PID controllers can be used for supervisory controller by cascade control, they do have a limitation

in that decoupled SISO pairing does not effectively handle interactions among loops. In addition, it is difficult to address the constraints and rate of changes for input-output. Model predictive control is an important multivariable centralized control strategy, which is an advanced control technique that takes advantage of the model's inherent ability to predict system behavior into the future. The appropriate control action depends on the dynamic characteristics of the plant, so the plant model is identified to predict the response of the output to an input sequence. In this thesis, plant model was represented by a state space form [43], which is compact and convenient for representing multivariable systems. For developing control model, relevant process input and output variables were first identified. In the first stage of the process, off-gas composition and flowrate are changed by the operating conditions of FLASH (flash drum). If so, temperature controller of flash drum can adjust the flash temperature by manipulating the heating utility. The temperature controller of the pre-cooler adjusts the cooling utility on the vapor feed stream of packed desorption column. These lead to a change in the product purities and feedback signal is sent to the split flowrate controller, which manipulates the amount of recycle flowrate. Because the HCl separation column is sensitive to changes in the manipulated variables, the set-points of column controller were not used as manipulated variables for process operability in the supervisory control. All the columns have a 6-minute time delay for the composition analyzer to measure H_2 and HCl impurity. The state space model was obtained by a step response test. The steps were in the following sequence for (MV1, MV2, MV3): (95, 100, 100) (95, 95, 100) (95, 95, 95) (97.5, 97.5, 95) (97.5, 97.5, 97.5) (100, 100, 100) (100, 100, 95)

(95, 95, 95). Fig. 14 shows the simulator responses to different combinations of step changes in the manipulated inputs (split flowrate [MV1], flash drum temperature [MV2], pre-cooler temperature for H2 feed [MV3]) and controlled outputs (H_2 purity [CV1], HCl impurity [CV2]). These input-output data in the form of time-series data were used to determine an approximate linear state space model for MPC design.

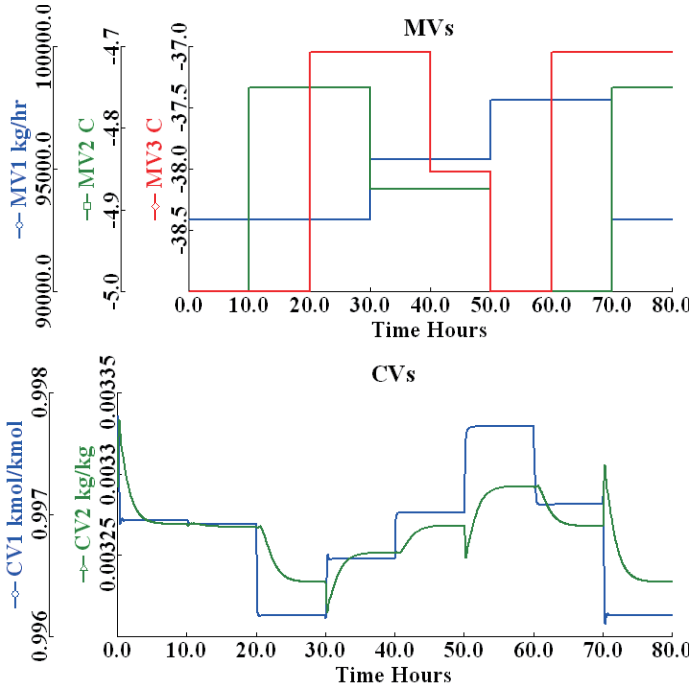

Figure 14: Responses to various supervisory layered step inputs for system identification

Using MATLAB's System Identification GUI Tool, where different algorithms and model orders were used on a trial and error basis, N4SID [44] showed the best fit to the plant data. Fig. 15 shows the

identification results using N4SID. The fitting accuracy was 94.4 % for CV1 and 60 % for CV2. A fitting accuracy for CV2 is about 60 %, which has the target value of 0.0033 mass impurity level. Because the scale of CV2 is 1e-3 in Fig. 15, 60 % of accuracy is enough to describe the system.

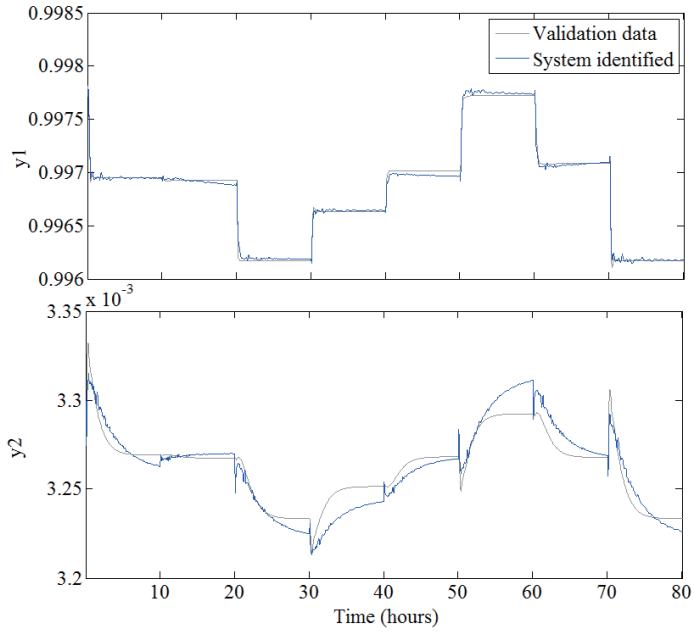

Figure 15: Comparison of system-identified step response models to plant model data

For testing MPC as a supervisory controller, we linked the relevant control input-output variable from Aspen Dynamics^{TM} Fig. 16 to the MATLAB/SIMULINK programming environment Fig. 17. The sample time of MPC was 3 min, and a prediction horizon of 80 and a control horizon of 4 were chosen. It takes eighty hours for one cycle of CVD operation, and the process shows a slow response. Therefore, the prediction horizon is 80 steps, which is large enough to make the

controller performance insensitive to further increase of the prediction horizon. Sample time of MPC was only 3 mins, and the control horizon was 4 hours, which is relatively small to reduce computational burden.

4.4.2 Case3. MPC based supervisory control

As demonstrated in Sec. 4.3.2, buffer tanks help reducing the flowrate disturbance except H_2 rich stream of vapor phase. In this case study, supervisory control structure was tested without the use of any buffer tanks. The centralized MPC was examined as a supervisory controller. The conditions of physical constraints on the input-output variables as in Table 2. The manipulated variables were the set-points of the PI controllers, and the values were optimized to satisfy the constraints while optimizing the objective by the MPC. The objective of the MPC is set as follows:

1. Molar purity of recovered H_2 (CV1): 0.9977
2. Mass impurity of recovered HCl (CV2): 0.0033

The cost function J is a sum of squares:

$$\begin{aligned} J = \sum_{i=1}^{p} \left(r_{k+i} - \hat{y}_{k+i|k}\right)^T W^y \left(r_{k+i} - \hat{y}_{k+i|k}\right) \\ + \sum_{i=0}^{m-1} \Delta u_{k+i}^T W^{\Delta u} \Delta u_{k+i} \\ + \sum_{i=0}^{m-1} \left(u_{k+i} - u_{n,k+i}\right)^T W^u \left(u_{k+i} - u_{n,k+i}\right) \end{aligned} \tag{4.2}$$

Figure 16: Process flowsheet in Aspen Dynamics for MPC

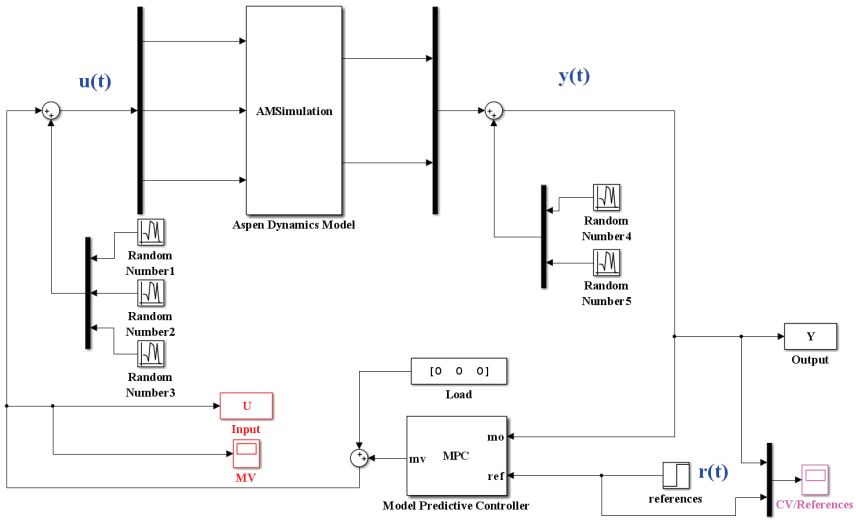

Figure 17: Simulink block diagram interfacing for off-gas recovery process

where, r_{k+i} is the set-point, u_k is the control action, $u_{n,k}$ is the nominal target of input. W^y, $W^{\Delta u}$ and $W^{\Delta u}$ are weighting parameters. $\hat{y}_{k+i|k}$ is the model prediction at $\left(k+i^{th}\right)$ time-step given the plant output until the k^{th} time-step. The cost function was minimized along with the input, input rate and output constraints as given in Eq. (4.3).

$$\begin{aligned} u_{min} \leq u_{k+i} \leq u_{max} \\ \Delta u_{min} \leq \Delta u_{k+i} \leq \Delta u_{max} \\ y_{min} \leq \hat{y}_{k+i|k} \leq y_{max} \end{aligned} \tag{4.3}$$

Because there is no reason to hold a particular MV at a nominal value, weights for MVs were set to small values close to zero (MV1: 0, MV2: 0.0001, MV3: 0). Since the absolute values of MVs have two orders of magnitude differences, the rate weight for MV1 is reduced

more than other MVs by a factor of 1000. In previous case study in Sec. 4.3, H_2 stream as a vapor phase incurred a control issue. Therefore, the weight of CV1 is increased more than CV2 in order to regulate it tightly.

Table 2: Constraints on input and outpu variables

Variable	Constraint		Rate constraint		Weight	Rate weight
	Min	Max	Min	Max		
MV1 (kg/hr)	87831	107831	-100	100	0	0.0001
MV2 (°C)	-10	10	-0.05	0.05	0.0001	0.1
MV3 (°C)	-49	-29	-0.05	0.05	0	0.1
CV1 (kmol/kmol)	0.997	0.999			100	
CV2 (kg/kr)	0.0023	0.0043			0.1	

Composition analyzers with 6-minute time delays were installed to identify the purity of the products. In Fig. 18, (a) and (b) show the movement of the MVs, and (c) and (d) are the results that the CVs were operated within the constraints despite periodic disturbances. It took approximately 140 hours to stabilize the entire process because of the sequential operations. After the stabilization, the entire process reached a cyclic steady state. When the H2 purity (c) decreased, the HCl purity (d) increased because the impurities such as HCl in the recovered H_2 were less separated, so they were recycled. Periodic disturbances, especially the effluent flowrate (f), influence all the units of the process; hence, to reject the disturbance, the MPC varied the recycle flowrate (MV1). When the effluent increased, the

recycle flowrate also increased for the higher HCl purity, and when the H_2 purity decreased, the temperature of the flash drum (MV2) and pre-cooler temperature for the H2 feed (MV3) decreased for the higher H_2 purity. Though the presence of flowrate disturbance unlike Sec 4.3.2, TC of HCl separation column (g) was well regulated by the centralized MPC. For the results, the purity of the recovered H2 and HCl were kept within the active constraints, though the reboiler duty of the HCl column (h) is slightly increased by 1.6 % because of the increased recycle flowrate (MV1). The proposed MPC-based supervisory control continuously adjusted the operating conditions such as the MVs (set points of PI controllers) that were fixed during the process design step and effectively rejected periodic disturbances.

4.4.3 Case4. MPC based supervisory control + buffer tank

It was shown that the MPC could control the CVs within the active constraints, and it was also found that a buffer tank could reduce the plant oscillations. This section examines the MPC with a buffer tank installation. Fig. 19 shows similar results in Sec 4.4.1 that the MPC worked well, and the plant oscillations were reduced in (a) (g). However, after 140 hours, the reboiler duty of the HCl column (h) had a lower variation compared with the MPC only case (Sec 4.4.1), while rejecting the flowrate disturbance by buffer tanks. The reboiler duty only increased by only 0.7 %, but the maximum heat duty decreased from 14 GJ/hr to 12 GJ/hr. This will also allow the heat exchangers to be of smaller size for the recycle flow in the recycle loop. From these results, if we use a supervisory controller based on the MPC with a

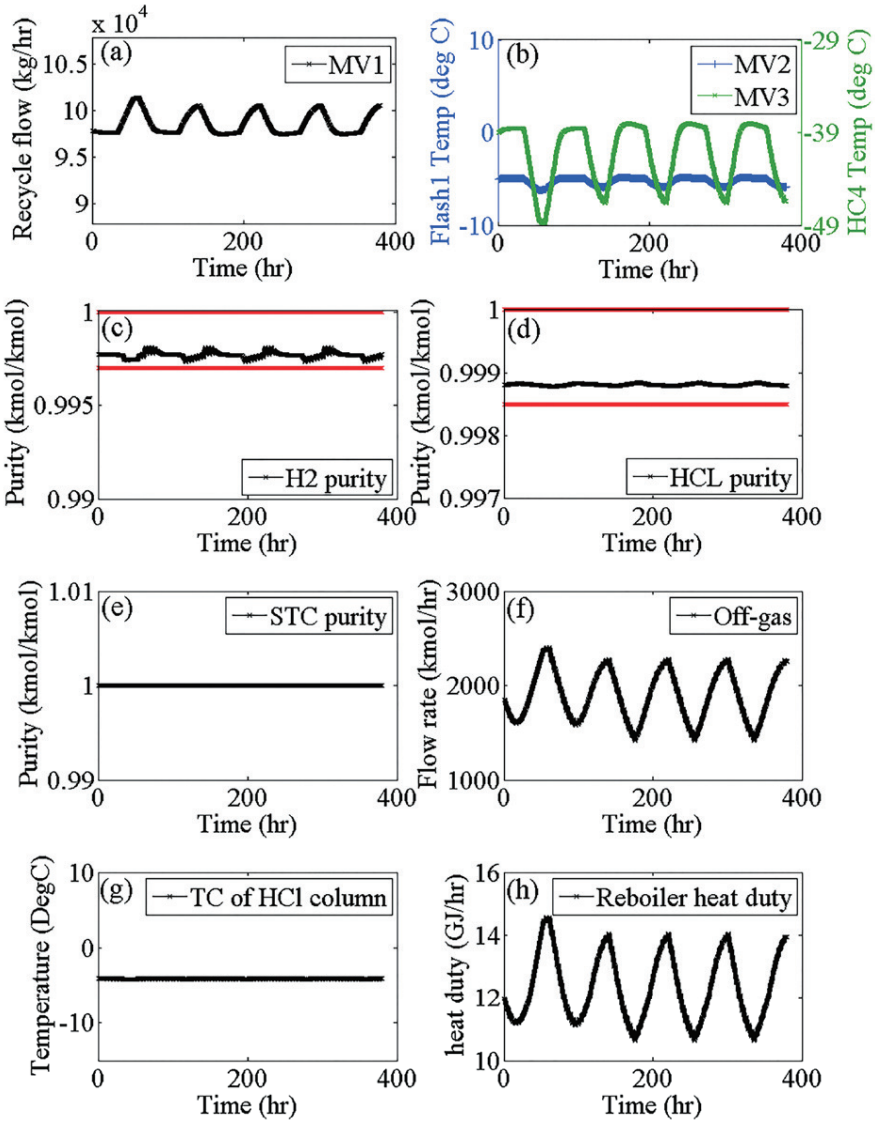

Figure 18: Performance of supervisory control

buffer tank for the process with periodic disturbances, not only can the process objective be accomplished, but the capital cost can also

be reduced within the constraints.

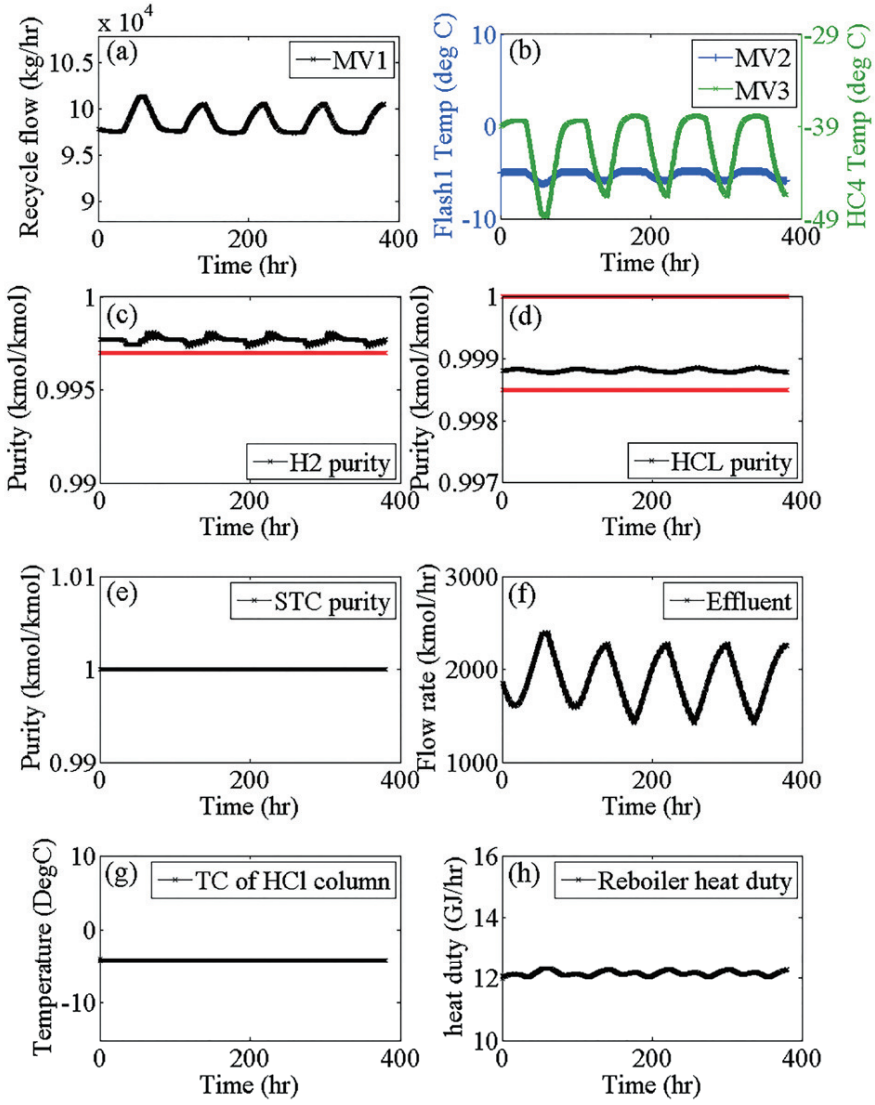

Figure 19: Performance of supervisory control with buffer tank

4.5 Comparison of four control schemes

In order to reject the periodic disturbances, four cases of different control schemes were considered for the off-gas recovery process. In Section 4.3, conventional fully decentralized PI controllers were implemented and they did not ensure the product purity even with buffer tanks. If the periodic disturbances existed only in liquid phase, installation of a buffer tank suffices. However, disturbance of gas phase exists in the process. In addition, if the product purity should be changed by a plant schedule, it is not easy to adjust the regulatory controllers (SISO-PI controllers) under the complex interactions among the equipment. On the other hand, MPC based supervisory controller effectively solved these problems in Sec 4.4. Using the identified plant model, supervisory controller handled the multivariable control problem with interactions and constraints in order to meet the product purity without a buffer tank. A comparison results between the PID and MPC controllers is listed in Table 3. During the one cycle (eighty hours), the advantage of supervisory controller over PID controllers is obvious. The difference in the integral squared error (ISE) is two orders of magnitude and CASE 3 has the lowest possible ISE under periodic disturbances. A buffer tank is shown to be an option not for the process operability but for the process economics and safety.

Table 3: Comparison of integral squared errors

CASE	Control scheme	H_2 separation	HCl separation
CASE 1	Fully decentralized PID controllers	3.76E-03	7.80E-04
CASE 2	Fully decentralized PID controllers with buffer tanks	3.79E-03	1.67E-04
CASE 3	MPC based supervisory controller	4.02E-05	4.60E-06
CASE 4	MPC based supervisory controller + buffer tanks	4.08E-05	8.08E-06

4.6 Case studies of the unexpected disturbances

4.6.1 Case5. Change of reactor operation intervals

In the polysilicon plant, some of the CVD reactors can be shut down during the deposition process, and the production schedule can be changed by the production target. Hence, developed control scheme adapted in CASE 3 should also have the robustness under unexpected abnormal situations. In the maintenance period for CVD reactor operation, the polysilicon product is manually collected, and the reactor is reset to the initial condition. This work requires man-hour shifts and time consumption. The task is planned by production schedules, and it can be adjusted according to the production target. When the turn-on intervals are changed from 4 hours to 5 hours, the flow patterns of the integrated off-gases are also changed. With this flowrate and composition change, developed control scheme in CASE 3 shows a good performance, as shown in Fig. 20. The reboiler duty was only increased by 0.6 %. The longer intervals makes the off-gas flowrate to be loosen, and it affects all parts of process then, leads to reduced

reboiler duty at the maximum point from 14 GJ/hr to 13 GJ/hr.

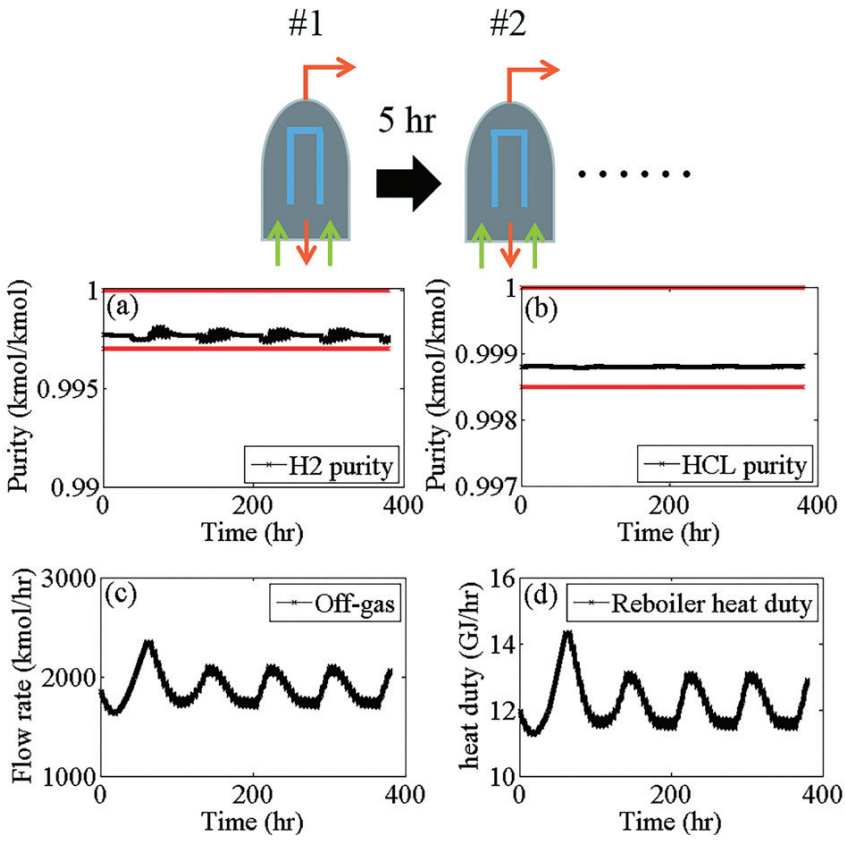

Figure 20: Supervisory control with interval change

4.6.2 Case6. Reactor shut-down case

In the CVD reactor operation, one of the most important things is to grow the polysilicon uniformly on the surface rod. If the deposited polysilicon is not uniform, it may contact the neighboring silicon, leading to short-circuiting and the break-down of the reactor. In this unexpected situation, after 4 hours, the CVD reactor can be restarted

again using a back-up reactor at 100 hr. At the results, developed control scheme in CASE 3 shows a stable performance in Fig. 21. The reboiler duty was only increased by 2.1 % because the off-gas flowrate and composition were changed.

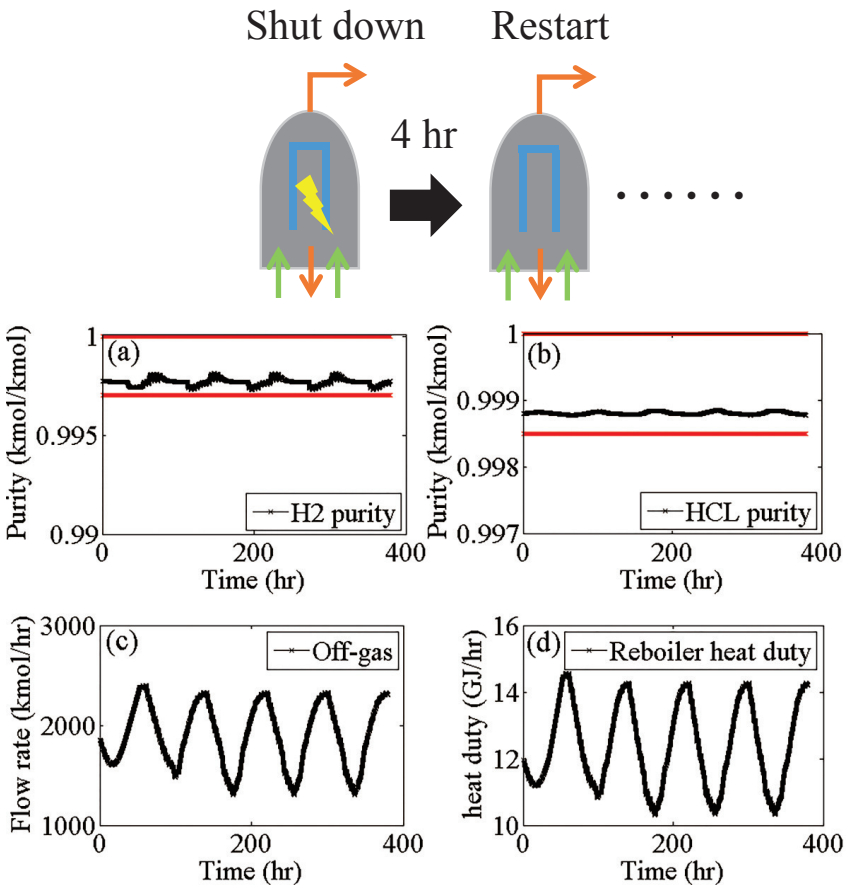

Figure 21: Supervisory control with reactor shut-down

4.6.3 Case7. Increasing hydrogen purity

Finally, control scheme adapted in CASE 3 was tested for the case in which the purity of the H2 was increased from 99.77 % to 99.87 % but the HCl purity was fixed. After 45 hours, H2 purity maintained a level of 99.87 %. Increasing the H2 purity caused a low HCl purity, so the recycle flowrate was increased to recover HCl. As a result, the reboiler heat duty was increased by 11.8 % as shown in Fig. 22.

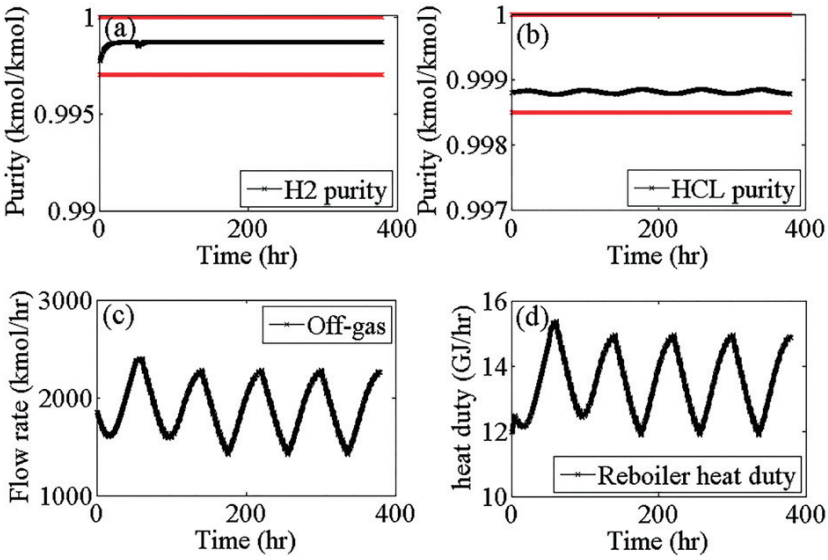

Figure 22: Supervisory control with increased H2 purity

4.7 Conclusion

The four cases of different control schemes for the process with periodic disturbances from batch parallel reactors was studied in this

chapter. It was found that conventional decentralized PI controllers were not sufficient for dealing with periodic disturbances effectively. Especially, process with gas phase stream cannot use a buffer tank, supervisory control based on MPC had better performance. Even though, proposed control strategy demonstrated a stable operation in the cases of discrete change of disturbances such as turn on intervals, reactors shut-down, and product purity. As discussed in Sec 4.4, proposed control scheme is enough to meet the product specification, buffer tank could reduce the plant oscillation and it can make the heat exchangers to be smaller in the recycle loop. Therefore this study suggests the use of buffer tank as well as supervisory controller, and they should be applied again in the process design stage. It is thus expected that the developed control strategy will be able to achieve the design of batch-continuous processes with periodic disturbances.

Chapter 5

Application of dividing wall column in silane off-gas recovery process

5.1 Introduction

In this chapter, design and control of dividing wall column was investigated in the separation of the silanes in order to maximize thermal efficiency. The recovered silanes are consist of DCS, TCS, and STC. In the previous chapters, silanes were separated into two streams of DCS and TCS to STC. According to patent of "Method for manufacturing polysilicon" [45], adjusting a ratio of DCS to TCS in the CVD reactor inlet can be used to prevent meltdown during the growth of silicon rod and to shortly manufacture a polycrystalline silicon rod having a diameter of 150 mm or larger with a minimal consumption of energy, and thus it is advantageous in terms of productivity and energy efficiency. It is thus that DCS and TCS is necessary to be separated, then to be adjusted their ratio into the reactor. In the separation of multicomponent, (for example, ternary mixture in this thesis), at least two columns are necessary for instance the direct (most volatile component is separated first) and indirect (the heaviest component is separated first) sequences shown in Fig. 23 [46]. The column (c) in Fig. 23 called "Petlyuk" configuration [47]

which is thermally coupled that the liquid and vapor leaving the first column are directly connected to second column. The first column (pre-fractionator) has no condenser and reboiler, and second column (main-column) has only one each of the required condenser and reboiler. This is not limited only to three component mixtures [48]. The pre-fractionator of the Petlyuk configuration performs a split between A (light boiling component) and C (heavy boiling component), while B (middle boiling component) is distributed between the top and bottom products. On the top of pre-fractionator column, C is almost never exited and further separation is occurred in the main-column between A and B, and B and C. It has been shown that the improvement in thermal efficiency leads to the saving of about 30 % as compared to the sequential distillation [14].

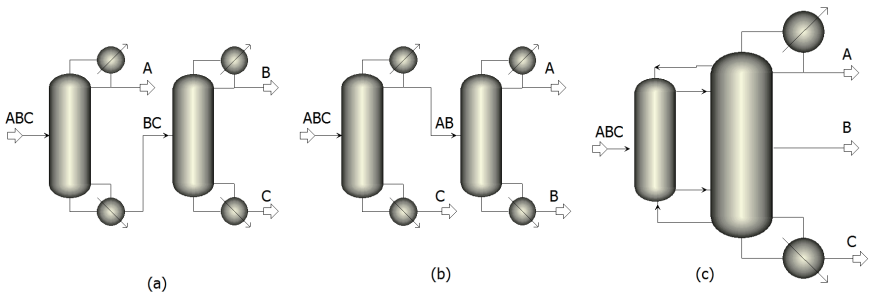

Figure 23: Distillation sequence for three components; (a) direct (b) indirect (c) Petlyuk column

The Petlyuk configuration is a good concept, however it is not easy to operate in practice. The liquid flow on top and the vapor flow of bottom in pre-fractionator cannot be controlled, even though pressure problems. Many researchers [49, 46] are tried to implement the Petlyuk concept, then dividing wall column (DWC) was invented.

The concept of DWC is simple that Petlyuk concept is implemented in a single distillation tower using internal wall as shown in Fig. 24, but the simulation is not easy due to the large number of design parameters. The first industrial application of a DWC was accomplished in 1985 by BASF SE at Ludwigshafen, Germany [49, 50]. Then, the BASF SE dominates the installation of DWC. There has been reported that the increase of DWC patents and application [46, 51, 52], over 50 DWCs were installed in 2006 (almost by BASF SE at that time), and over than 100 DWCs were operating in 2010 (worldwide). On the other hand, there are limitations in the DWC application. The operational pressure variation between column sections is impossible, and there is high temperature difference between reboiler and condenser, also DWC has greater column height compared with conventional columns. Therefore, it is necessary to design the DWC cautiously.

In this chapter, DWC was applied for the separation of the silanes to DCS, TCS, and STC. Conventional direct sequential columns were first designed and optimized, and then compared them with DWC column. With the optimized DWC design, further studies were performed to implement the control structure. Design and optimization were implemented in Aspen Plus^{TM} environment using steady-state model, and the comparison of control strategies for DWC was performed with rigorous dynamic model using Aspen Dynamics^{TM}

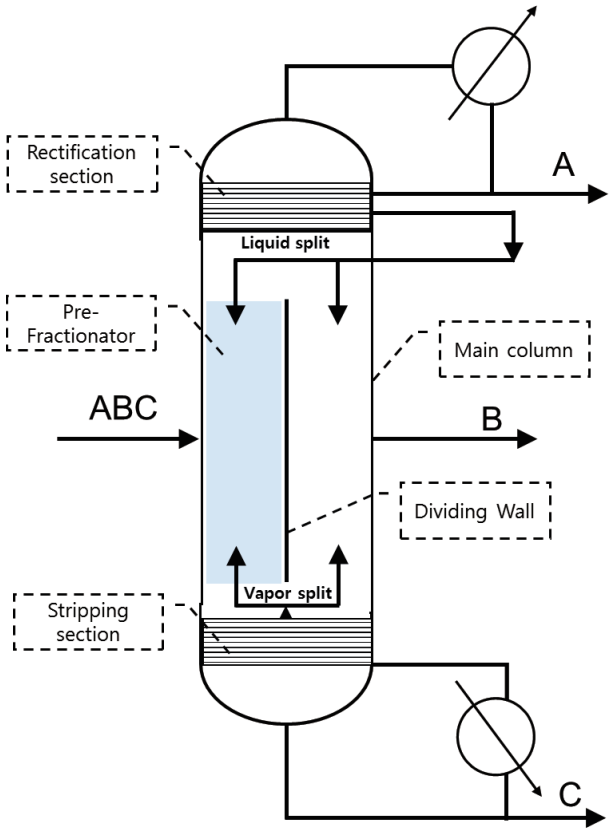

Figure 24: Schematics of a DWC

5.2 Design and optimization of direct sequential configuration

Ternary mixture which has the relative volatilities that DCS, TCS and STC are 1, 1.9 and 3.4. In this section, conventional direct sequence of columns were designed in two steps. The conceptual design of the columns was performed in a shortcut model, then rigorous model was applied to satisfy the product specifications. There are

two columns for the separation of silanes, one recovered DCS and the other separate the TCS and STC sequentially as shown in Fig. 25.

At first, shortcut method was used to determine the total stage of columns. In a shortcut method, unit operation is designed for single feed, two product distillation processes. For a specified product recovery (both light and heavy), the shortcut column first estimates the minimum number of stages and the minimum reflux ratio, and then it calculates the required number of theoretical stages based on the specified reflux ratio. The optimum feed stage location and the condenser and reboiler duties are also estimated, however these values should be calculated again in a rigorous mode of distillation model because shortcut method assumes a constant relativities and constant molar overflow. The calculated results are shown in Table 4. Using this information, initial values were applied to the rigorous distillation model.

Table 4: Simulation Results of shortcut method

Results	Short1	Short2	Unit
Minimum reflux ratio	1.56	7.38	
Actual reflux ratio	2.5	8.49	
Minimum number of stages	19.29	15.16	
Feed stage	31.65	30	
Number of actual stages above feed	20.4	21.2	
Reboiler heating required	26.8	10.6	GJ/hr
Condenser cooling required	27.5	9.6	GJ/hr
Distillate temperature	56.9	47.4	°C
Bottom temperature	102.2	83.3	°C
Distillate to feed fraction	0.64	0.14	

In the rigorous model, in order to meet the product specification, DESIGN SPEC and VARY should be justified. DESIGN SPEC

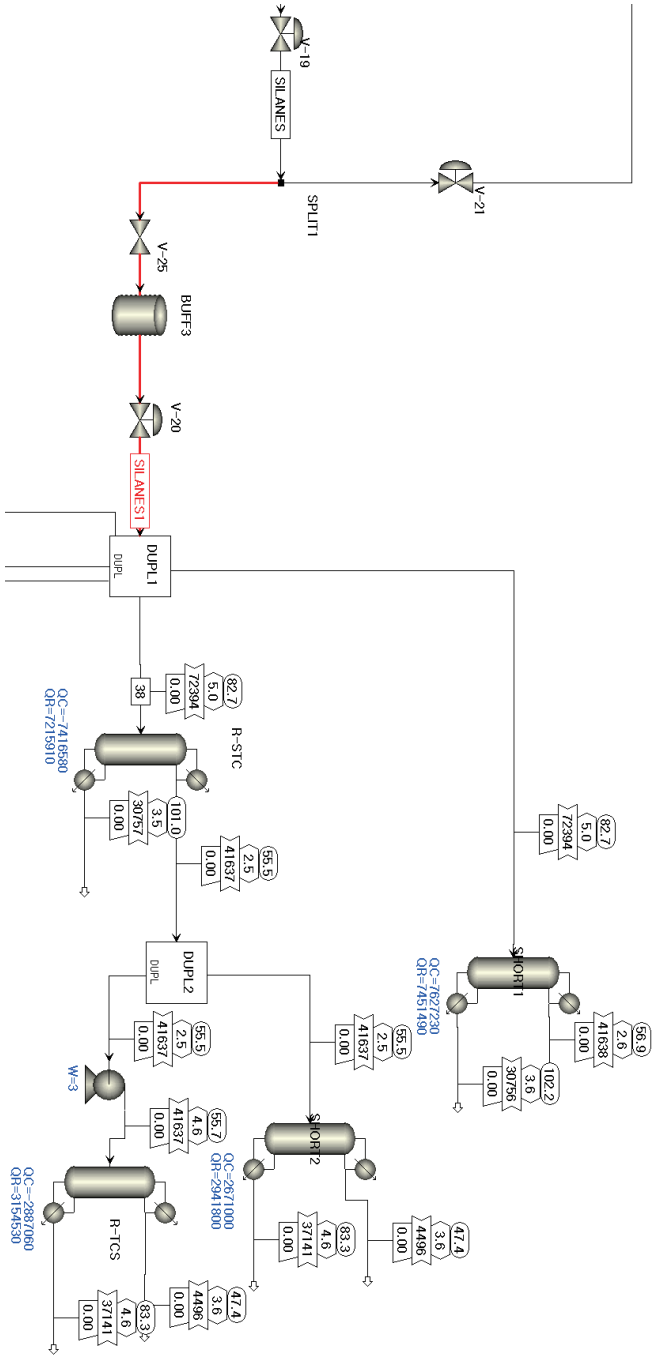

Figure 25: Design of direct sequential column

means a target, and VARY is manipulated variable to obtain the target result. The purity of recovered purities set to be the same of 99 mol % in each of silanes varying with each column of reflux ratio (the ratio of reflux rate to distillate). Keeping with a DESIGN SPEC, sensitivity analysis was performed to determine the feed tray location. As listed in table 5, feed tray location of 23 has the lowest required reboiler heat duty to separate the STC, and location of feed tray at 16 also has the minimum required heat duty to recover TCS. The total required heat duty is optimized to 10.37 MW (37.33 GJ/hr) in the base case design.

Table 5: Simulation Results of shortcut method

R-STC		R-TCS	
FEED STAGE			
	Watt		Watt
16	9654505	10	4414792
17	8919434	11	3862540
18	8369795	12	3536227
19	7953972	13	3339728
20	7643011	14	3226062
21	7418531	15	3169763
22	7275431	16	3154533
23	7215906	17	3170951
24	7253572	18	3213618
25	7422135	19	3280453
26	7805741	20	3372326
27	8599339	21	3493723
		22	3652347

5.3 Design and optimization of DWC

There has been many attempts to implement the DWC design [51]. Because there is no available distinct model in commercial process simulators, researchers has been used the combination of existed models indirectly. Several approaches can be used, ranging from one to four column models as a sequence of column sections. One column pump-around models can be used to simulate the DWC with simple computation, however it was reported that it can lead to convergence problems as the entire vapor and liquid are drawn off in two points of the column, and nothing remains to flow to the next tray [53, 51]. Two column sequences are possible, and they can be easily set-up with more flexibility than the pump-around model, however vapor and liquid split ratio is not ratio but flowrate that is not adequate to simulate the dividing-wall in rigorous dynamic simulation. Four columns sequence model is the most suitable to simulate the DWC. As shown in Fig. 26 (c), there are four columns: left side one is pre-fractionator (feed side section), right side one is product column (side middle-product), top side one is rectifying section (light product), bottom side one is stripping section (heavier product). Four column configuration allows for maximum flexibility with regard to specifications for different column sections, as well as vapor and liquid splits, it is the most suitable for dynamic simulation though it is not easy to converge the simulation.

The optimization of DWC is more difficult than design because the estimation of the number of stages in each section is an integer variable, column optimization problem is a class of mixed integer non-linear programming problems (MINLPs). Dünnebier and Pan-

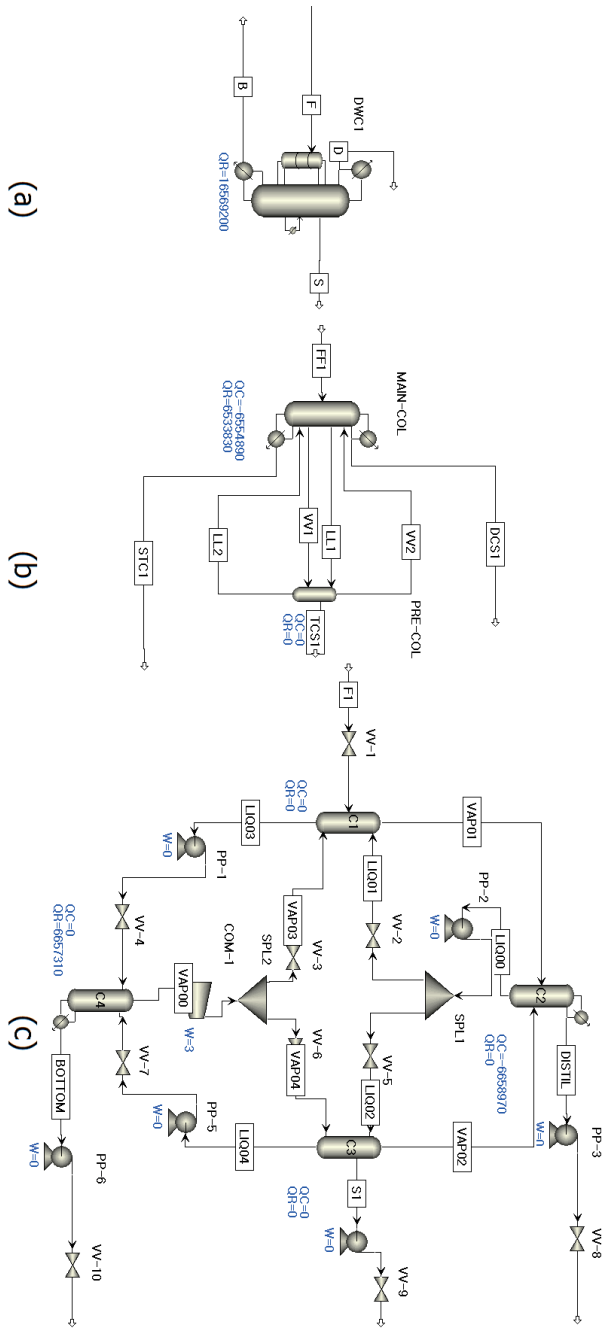

Figure 26: Various sequence method of DWC in Aspen Plus ((a) MultiFrac model; (b) two columns sequence model; (c) four columns sequence model

telides [54] was proposed the superstructure of column using local optimization code (CONOPT) and commercial simulator (gPROMS), however they found only local optimum. Wenzel and Rohm [55] have presented a method for simultaneous design and optimization using an external optimization routine with Aspen Plus^{TM}. Kiss et al. [56] also studied similar research that the optimal design of a reactive DWC using Aspen Plus^{TM} and MATLAB. In this thesis, general and simple approach is proposed for the optimal design and control of DWC. As shown in Fig. 27, proposed method is consist of 5 steps for the steady state simulation.

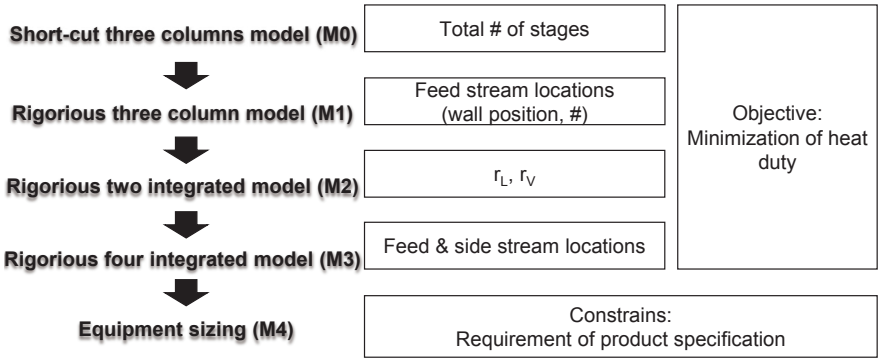

Figure 27: Proposed method for DWC design

By the novel scheme, conventional direct sequence columns (called "M0" in this thesis) were design using short-cut method to find the required total stages for each column while meeting the product specifications. The target of product set to 0.99 mol-% for each of DCS (14 stages), TCS (16stages), and STC (31 stages). It is noted that the heavey component should be minimized in the top vapor product of first column to enhance the energy efficiency by avoiding the remix-

ing of intermediate component. In the second step, rigorous three distillation columns (called “M1” in this thesis) were designed and optimized to obtain the minimum energy consumption using three columns. In order to meet the product specification, the reflux ratio, side stream flowrate, and reboiler duty was manipulated varying with locations of feed stream. The first column is pre-fractionator which should be designed to be non-heavier component in the top product. The second column distillates light product, while third one separates the heavier product. Varying with the feed tray location, the required total reboiler duties (Q1 + Q2 + Q3) were found and the results are in Fig. 28. Additionally, required height of wall and position can be determined at the lowest energy consumption.

In the third step, developed conventional three sequential columns was converted to two columns integrated model of DWC. The initial vapor and liquid stream from the pre-fractionator column can be estimated by the previous three sequential columns model (M1). The reflux rate of M1 acts like liquid flow from the rectification section, and the boil-up rate can be treated like vapor flow from the stripping section of DWC. And the composition of liquid and vapor from the pre-fractionator can be used for the initial values of stream to the main column. Using these values, two columns integrated model (M2) can be easily designed. The two columns integrated model is thermodynamically equivalent to a DWC as shown in Fig. 29, further optimization for the internal flow can be progressed because of better convergence than four integrated columns model.

Split ratio of vapor and liquid flow rate were determined by the amount of required reboiler duty varying with the values from 100 kmol/hr to 1200 kmol/hr, and the results are shown in Fig. 30. Be-

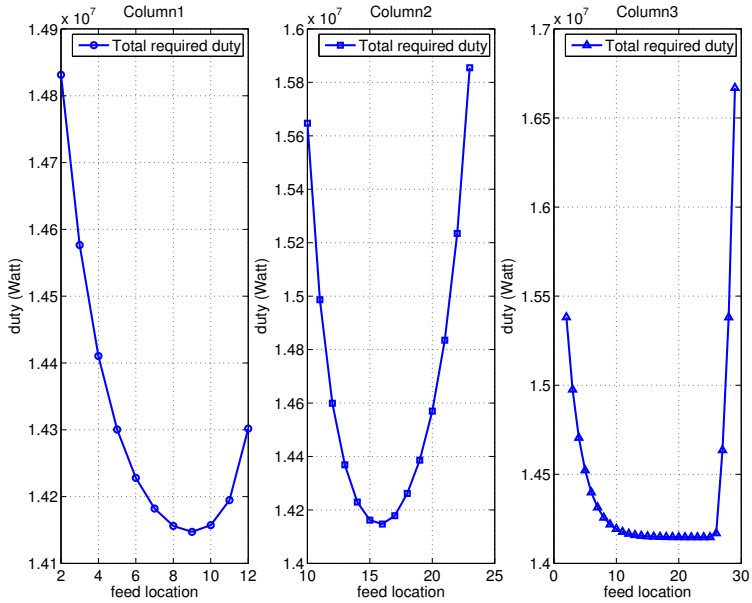

Figure 28: Optimization results of conventional three sequential columns model (M1)

cause it should be satisfied that the purity of products (DCS, TCS, and STC) are equal to the 99 mol %, infeasible region is existed. The optimum values were found 296 kmol/hr of liquid split rate, 410 kmol/hr of vapor split rate, and these values can be converted to mass ratio, 0.3 for liquid split ratio, 0.4 for vapor split ratio approximately.

In the fourth step, two column model (M2) was converted to four columns sequence model (M3) of DWC. The M3 is the closest model of practical DWC, therefore final optimization was performed to determine the location of feed and side product stream while vapor and liquid split rate was fixed from optimized values of M2. Varying with the locations of that, required reboiler duty was calculated, and the

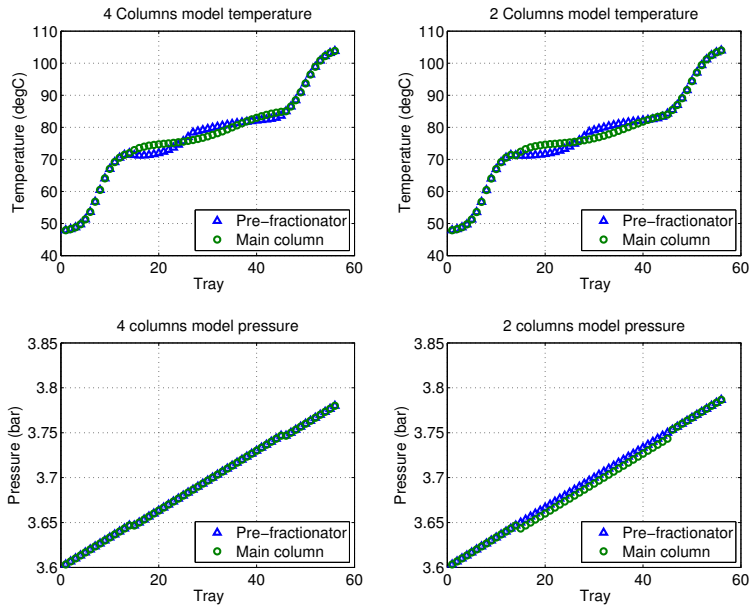

Figure 29: Comparison results between two and four columns integrated model

results are shown in Fig. 31. The total required heat duty is optimized to 6.66 MW (23.97 GJ/hr) in the four columns integrated design of DWC which is reduced energy consumption to be about 36 %.

In the final step, the equipment were sized for the column, reflux and reboiler sump drum. Tray-sizing tool of Aspen Plus^{TM} can conveniently calculate the column diameters. The size of condenser and sump drum can be calculated by the each of liquid stream flowrate at the top or bottom. The liquid hold-up was set to 20 min for 50 % of total, then the diameter and length was obtained by assuming a length to diameter ratio of two, the diameters and lengths can be calculated. The results are shown in Table 6. The column pressure drop was as-

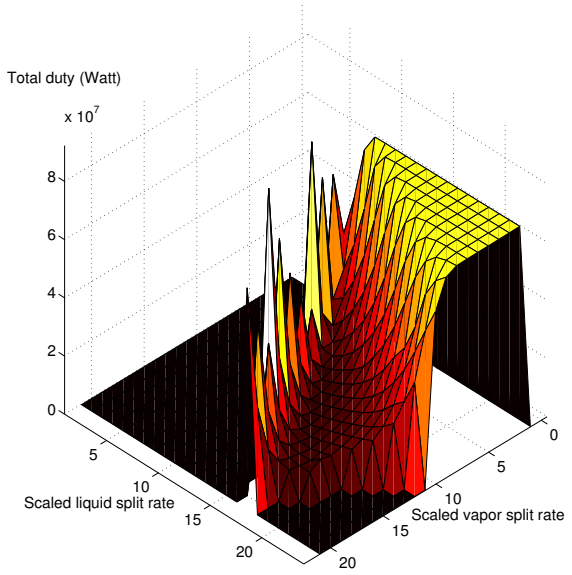

Figure 30: Optimization results of two columns integrated model of DWC (M2)

sumed 2.5 mmHg per stage. The packing column was used and its internal was GEMPAK 3A, HETP (Height equivalent to a theoretical plate) was assumed 0.4 meter. The maximum fractional capacity of column (Eq. (5.1)) is less than 0.62. Final structure of DWC design is shown in Fig. 32.

$$CS = VS\sqrt{\frac{\rho_v}{\rho_l - \rho_v}} \tag{5.1}$$

where, CS is the capacity factor, VS is superficial velocity of vapor to packing, ρ_v is density of vapor to packing, ρ_l is the density of liquid from packing.

The sequence of novel approach can be summarized briefly as

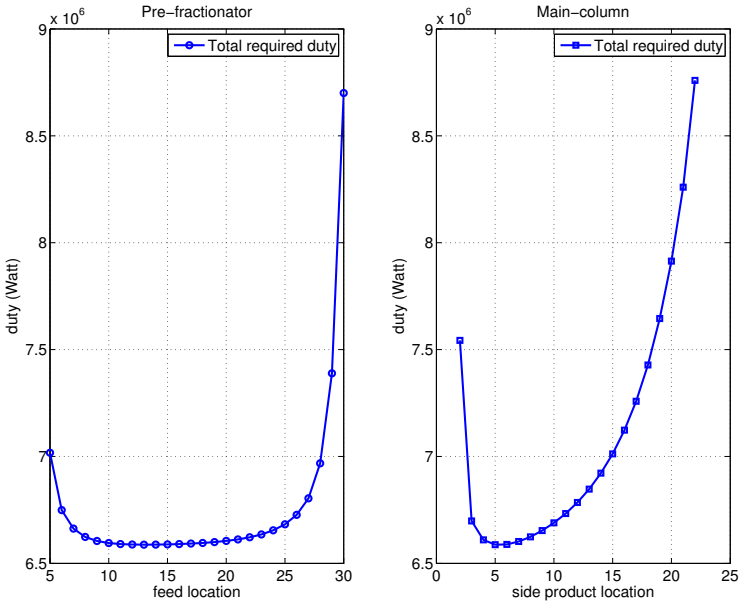

Figure 31: Optimization results of four columns integrated model of DWC (M3)

Table 6: Simulation Results of shortcut method

Equipment Unit	Dia. (m)	Fractional capacity	Flow on top (cum/s)	Reflux drum D (meter)	Flow on bottom (cum/s)	Sump drum D (meter)
Rectifier	3.3	0.43	0.026	2.72	0.029	2.81
Absorber1 (Feed)	2.09 (1.32)	0.61			0.026	2.69
Absorber2 (Side-product)	2.56 (1.98)	0.45			0.013	1.68
Stripper	3.3	0.53			0.007	1.71

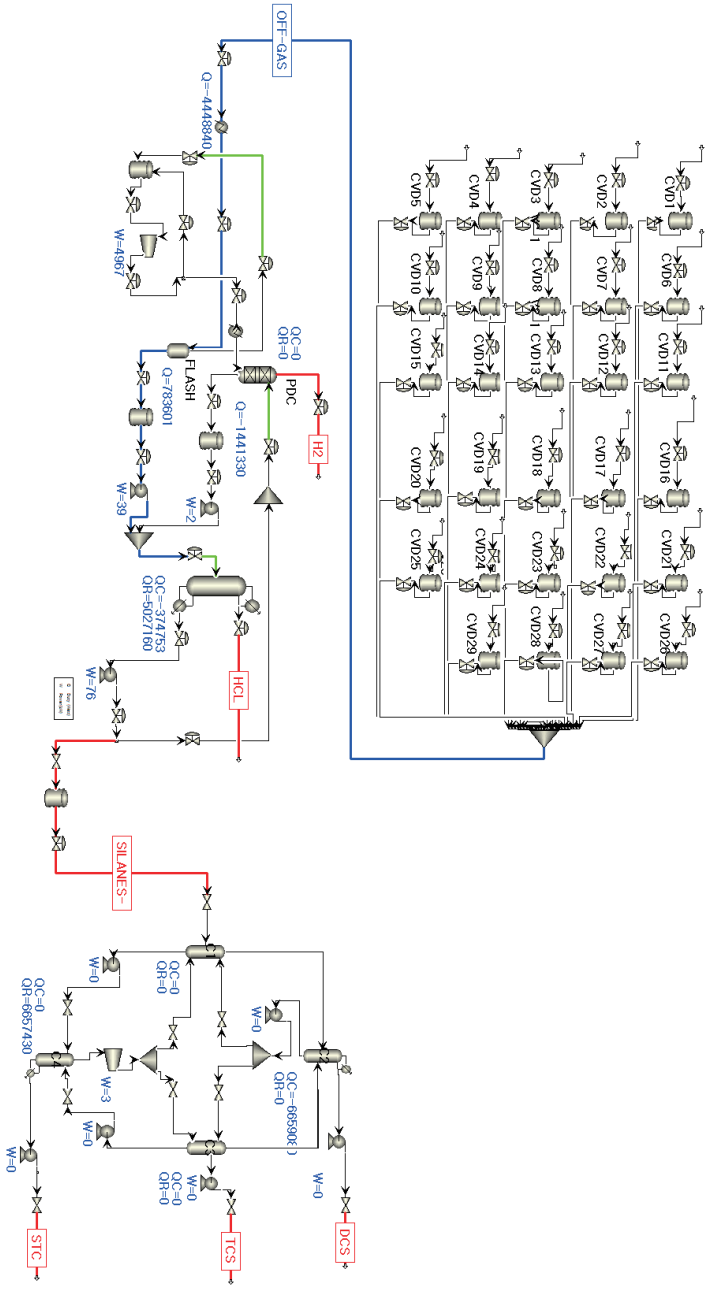

Figure 32: Final structure of DWC application

following: Conventional short-cut columns (M0) → Obtaining the total stage of columns → Convention sequential distillation column (M1) → Optimizing feed location, position and height of wall → two integrated columns (M2) → Optimizing r_L, r_V → Four integrated columns (M3) → Optimizing the location of feed and side stream → Equipment sizing → Dynamic model (M4)

5.4 DWC control case studies

In this section, the control scheme of DWC was investigated for a relevant operation. It has been demonstrated that the implicit optimization of energy consumption is achieved by controlling the heavy impurity at the top of the pre-fractionator [57, 58], however it is related to controllability properties of the system. There has been many researches which treat the control study of thermally coupled distillation columns [59, 60, 61]. The reliable and robust synthesis methods for DWC were suggested by an analysis of both thermodynamic and controllability [62, 63]. As a result, a good performance could be achieved for the thermally coupled distillation systems. Using previous demonstrations, three-point control structure and some four-point control structures were compared using an optimized four columns model of DWC. The steady state model of M3 was converted to dynamic model of M4. Before exporting the steady state file into Aspen Dynamics^{TM}, some changes to be considered in order to use a pressure-driven dynamic simulation. The valves should be installed between the vessels, and compensation units such as pump or compressors were also used for pressure drop from valves. The split ratio of liquid and vapor was implemented by controllers with remote set

points (RC1 and RC2) on cascade as shown in Fig. 33. The composition control loops each have a 5 minute of time-delay, and they were tuned using a sequential method. Relay-feedback tuning was used to fine the ultimate gain and period for each composition controllers (CC3 $\rightarrow$ CC1 $\rightarrow$ CC2 $\rightarrow$ CC4) as shown in Fig. 34. All cases were tested for the changes of feed flowrate by increases and decreases of 10 %.

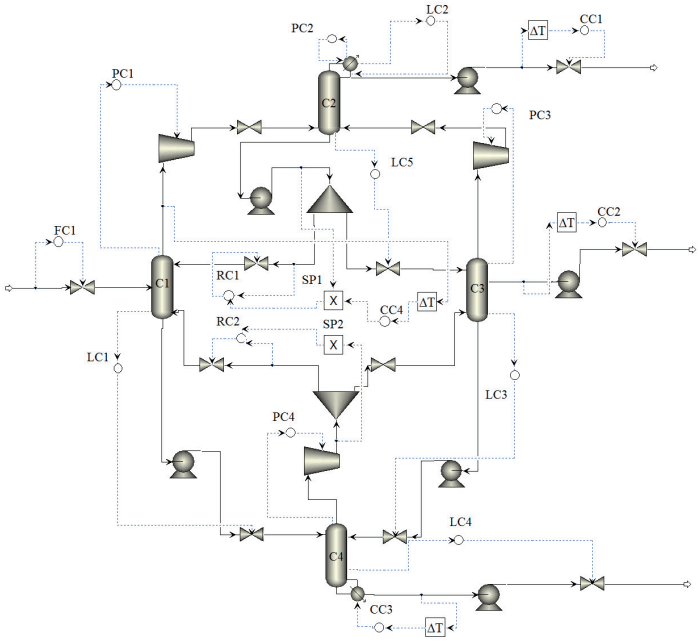

Figure 33: Dynamic model of DWC

5.4.1 Selection of control variables

The DWC system has 5 degrees of freedom (DOF), two DOF are originated from column, one is side flow, and rest of two are from the wall. Kiss et el [52] showed the flow relationships of DWC based on

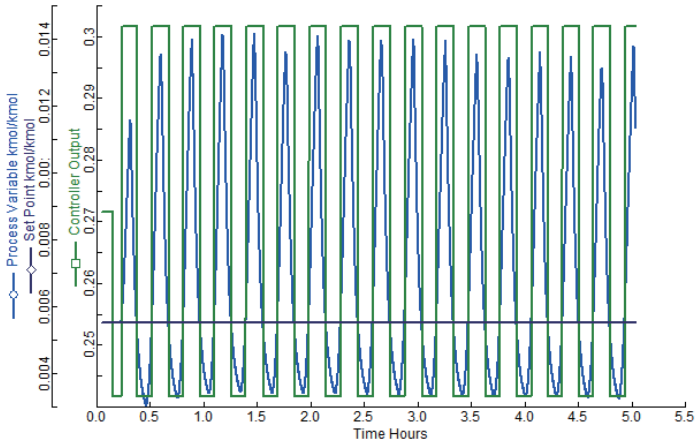

Figure 34: Relay-feed back tuning

the mole balance. They divided the DWC system to 6 sections, and the specification of L, V, S, r_L, r_V is sufficient to determine all the flowrates in the DWC. Table 7 shows the list of DOF in the DWC system. Among them, only 4 variables can be available to control, because vapor split ratio is already determined in the design step, it can not be used to control the column. thd distillate (D) and bottoms rate (B) are used to maintain the level of condenser and reboiler drum, and the condenser duty controls column pressure. The vapor boil-up rate (V) and reflux ratio (R) are equivalent to reboiler duty (Q_r) and reflux rate (L). Hence, the remaining DOF left (S, L, Q_r, r_L) can be used to control four variables. Typically, the purities of all three product should be controlled (three point control structure), and the remaining 1 DOF left can be used to achieve other objective (four point control structure). In the four point control structure, there are 4 combination of cases shown in Fig. 35, where Top-A denotes DCS in distillate, Side-A is DCS, Side-B is TCS, and Side-C is STC in side

flow, BTM-C is STC in bottom flow, yC is STC in vapor stream of pre-fractionator.

Table 7: List of DOF to DWC system

DOF	Description	Availability
D	distillate rate	liquid level in reflux drum
S	side stream rate	Available
B	bottoms rate	liquid level in rebolier sump drum
Q_c	condenser duty	column pressure
L	liquid reflux rate	Available
Q_r	reboiler duty	Available
V	vapor boil-up rate	equivalent to Q_r
r_L	internal liquid split ratio	Available
r_V	internal vapor split ratio	physically fixed
R=L/D	reflux ratio	equivalent to L

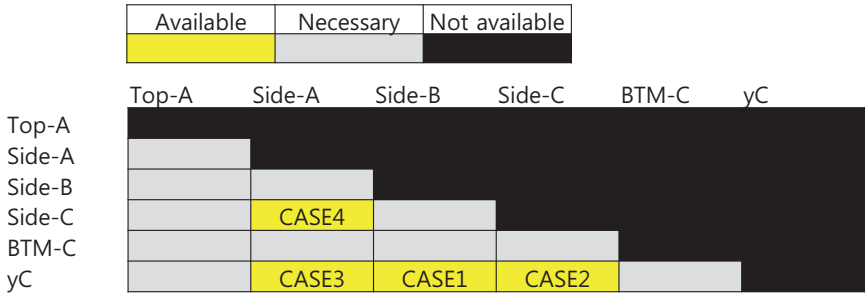

Figure 35: Combination of four-point control structure

5.4.2 Three-point control structure

The integration of two columns into one shell leads to more interactions among the controlled and manipulated variables. In this thesis, relative gain array (RGA) [64] was used to choose the best

control structure and determine the controllability. The relative gain array of the process is defined as: $\Lambda = G(0) \circ (G(0))^{-T}$, where $G(0)$ is the multivariable state space process model and $\circ$ denotes element-by-element multiplication, and M^{-T} denotes the transpose of the inverse of a matrix M. The RGA element is deifned the ratio of the open-loop gain to closed loop gain for a pair of variables. The elements in each column and low of the RGA sum up to 1. If one RGA value per column is close to 1 and the remaining elements are small, the interaction in the plant suggests a weak relationship. Conversely, one of the corresponding RGA valus is negative will suffer from the problem that the controller settings give an unstable system.

From the RGA analysis, three pairs of controllers were selected to control the all product purity as listed in Table 8, and it has been tunned three composition controllers as shown in Table 9. CC1 controls the DCS purity in distillate flow, CC2 controls the TCS purity in the side-product stream, and the CC3 regulates the STC in the bottom flow by manipulating the reflux rate, side-product flow rate, and reboiler duty. This is a base control structure of DWC system. There is one remained degree of freedom which is liquid split ratio, it can be used to optimize the process in four point control structure. The results are shown in Fig. 36.

Table 8: RGA results for three-point control structure

CV / MV	L	Q_r	S
D(DCS)	1.02	-0.02	0.00
S(TCS)	0.00	0.26	0.73
B(STC)	-0.02	0.75	0.27

Table 9: Controller parameters of three-point control structure

Controller	CV	MV	K_c	τ_I(min)	Action
CC1	x_D(DCS)	Reflux rate (L)	4.08	140	-
CC2	x_S(TCS)	Side-product flowrate (S)	48.33	63	+
CC3	x_B(STC)	Reboiler duty (Q_r	5.49	49	-

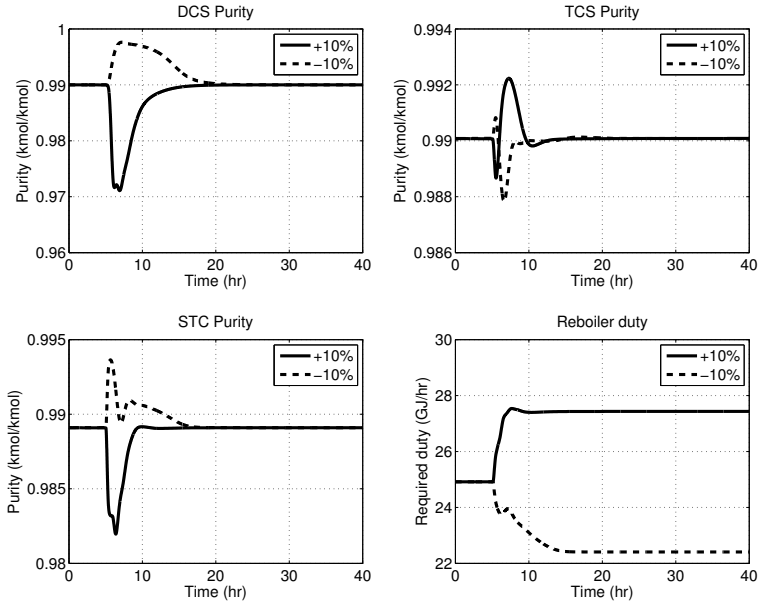

Figure 36: Results of three-point control structure

5.4.3 Four-point control structure-CASE1

With one degree of freedom (r_L, liquid split ratio), heavy componenet in the top of the pre-fractionator was controlled. The paring of MV and CV was selected by RGA analysis as shown in Table10. When the feed flowrate was decreased, the oscillation was occurred

and the settling time of DCS controller was longer than base case (three point control structure). The energy consumption during the period rejecting the disturbances was increased, because the settling time was longer than base case. The tunging parameters of controllers are listed in Table 11, and the control results are shown in Fig. 37.

Table 10: RGA results for four-point control structure-CASE1

CV / MV	r_L	L	Q_r	S
D(DCS)	-0.01	1.02	-0.01	0.00
S(TCS)	0.03	0.00	0.23	0.73
B(STC)	0.02	-0.02	0.74	0.27
yC	0.95	0.00	0.05	0.00

Table 11: Controller parameters of four-point control structure-CASE1

Controller	CV	MV	K_c	τ_I(min)	Action
CC1	x_D(DCS)	Reflux rate	3.58	148	-
CC2	x_S(TCS)	Side-product flowrate	84.61	97	+
CC3	x_B(STC)	Reboiler duty	5.73	48	-
CC4	x_P(STC)	r_L	0.06	39	+

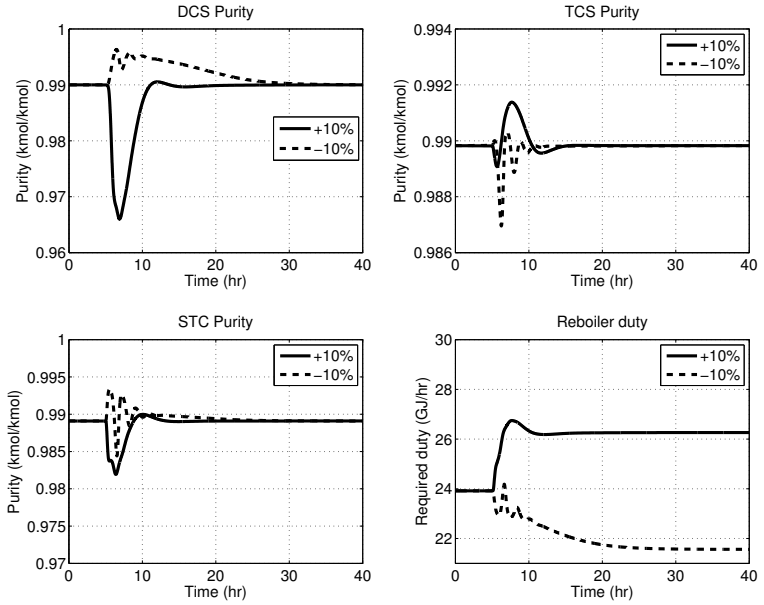

Figure 37: Results of four-point control structure-CASE1

5.4.4 Four-point control structure-CASE2

In this control structure, CV of CC2 was changed from TCS to STC purity in the side-product stream. Because the response of recovered DCS purity was sluggish and the oscillation was occured in previous control structure, heavy impurity in the side product stream was controlled would be expected a good performance by CC2. The controllers were tuned and the pairing of controllers are listed in Table 12 and 13. As shown in Fig. 38, this control structure provides improved control performances. The settling time is totally reduced by 33 % (15 hr $\rightarrow$ 10 hr)

Table 12: RGA results for four-point control structure-CASE2

CV / MV	r_L	L	Q_r	S
D(DCS)	0.00	1.01	0.00	0.00
S(SCS)	0.03	0.02	0.20	0.75
B(STC)	0.02	-0.02	0.75	0.25
yC	0.95	0.00	0.05	0.00

Table 13: Controller parameters of four-point control structure-CASE2

Controller	CV	MV	K_c	τ_I(min)	Action
CC1	x_D(DCS)	Reflux rate	5.79	122	-
CC2	x_S(STC)	Side-product flowrate	0.24	56	-
CC3	x_B(STC)	Reboiler duty	5.76	49	-
CC4	x_P(STC)	r_L	0.06	39	+

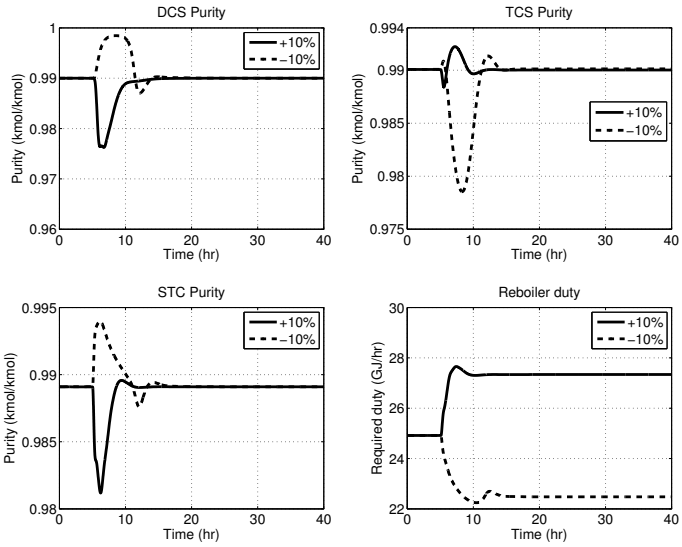

Figure 38: Results of four-point control structure-CASE2

5.4.5 Four-point control structure-CASE3

In this control structure, light impurity in the side product flow were controlled instead of heavy impurity (CASE2). As listed in Table 14, RGA analysis results shows that the interactions among controllers were increased. The tunning parameters of controllers are shown in Table 15. As a results, the performance of controllers was worse than three point control structure, especially, the settling time of controllers for DCS and STC was greatly increased, hence the energy consumption was also increased. This control structure shows more sluggish responses in Fig. 39.

Table 14: RGA results for four-point control structure-CASE3

CV / MV	r_L	L	Q_r	S
D(DCS)	-0.22	2.31	-1.27	0.17
S(DCS)	0.34	-1.33	3.03	-1.04
B(STC)	-0.20	0.02	-0.77	1.95
yC	1.08	-0.01	0.01	-0.08

Table 15: Controller parameters of four-point control structure-CASE3

Controller	CV	MV	K_c	τ_I(min)	Action
CC1	x_D(DCS)	Reflux rate	3.93	140	-
CC2	x_B(STC)	Side-product flowrate	26.18	88	+
CC3	x_S(DCS)	Reboiler duty	0.15	27	+
CC4	x_P(STC)	r_L	0.06	39	+

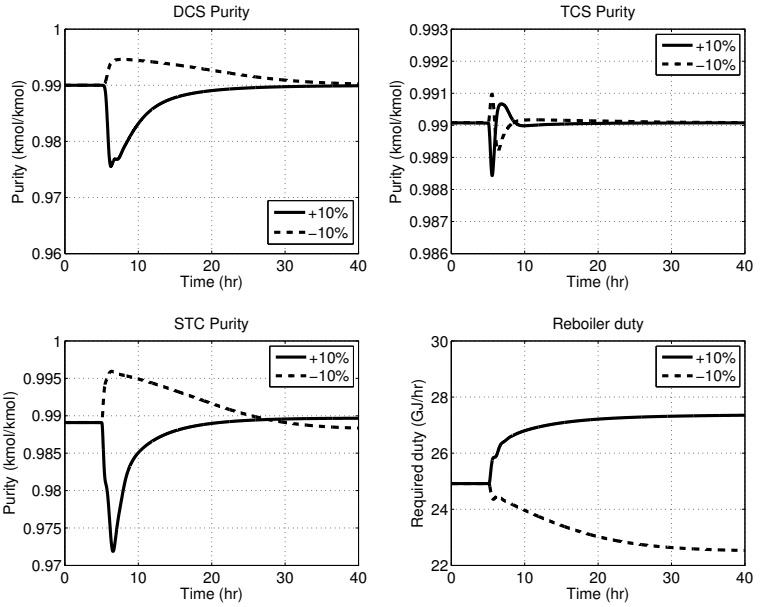

Figure 39: Results of four-point control structure-CASE3

5.4.6 Four-point control structure-CASE4

The CASE4 is constructed to control the both of light and haevy impurities in the side product flow, and the heavy product in the bottoms flow is controlled by liquid split ratio. The results of RGA analysis shows large interactions as shown in Table 16. The tunning parameters of controllers are listed in Table 17. As shown in Fig. 40, The purity of STC is well controlled, however response of DCS controller is sluggish and the purity of TCS does not reach the set-point until 40 hr.

Table 16: RGA results for four-point control structure-CASE4

CV / MV	r_L	L	Q_r	S
D(DCS)	1.62	0.81	-1.42	0.00
S(DCS)	-2.59	0.20	3.41	-0.02
B(STC)	1.70	-0.03	-0.96	0.29
S(STC)	0.27	0.02	-0.02	0.74

Table 17: Controller parameters of four-point control structure-CASE4

Controller	CV	MV	K_c	τ_I(min)	Action
CC1	x_D(DCS)	Reflux rate	3.24	149	-
CC2	x_S(STC)	Side-product flowrate	0.34	43	-
CC3	x_S(DCS)	Reboiler duty	0.18	29	+
CC4	x_B(STC)	r_L	0.26	96	+

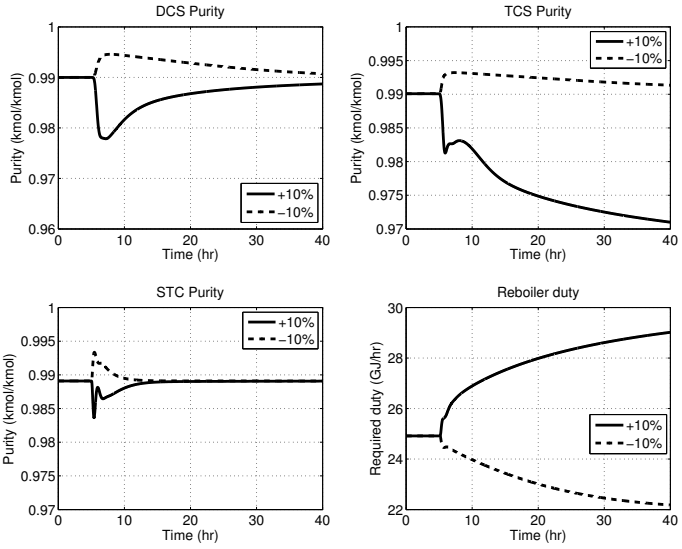

Figure 40: Results of four-point control structure-CASE4

5.4.7 Six-point control structure

The case studies of four-point control structure showed strong interactions between controllers in the DWC system. And the RGA analysis was effective method to select the controlled and manipulated variables. In this section, controled variables were expanded to six variables, including level controllers of reflux and reboiler drum. In the previous case studies, it was assumed that a level of condenser drum (H_T) is controlled by distillate rate and a level of reboiler drum (H_R) is controlled by bottoms rate. The results of RGA analysis for 6 by 6 are listed in Table 18. Though there are some interactions that the reboiler duty and side flow rate affect both purities of TCS in the side flow and STC in the bottoms flow, the performace of controllers shows the most stable and the settling time is also reduced at the same time. The parameters of controllers were tuned as shown in Table 19. The results are in Fig. 41

Table 18: RGA results for six-point control structure

CV / MV	r_L	L	Q_r	S	D	B
D(DCS)	0.01	0.01	0.01	0.00	0.97	0.00
S(TCS)	0.03	-0.01	0.31	0.70	-0.01	-0.03
B(STC)	0.00	0.02	0.53	0.19	0.03	0.23
yC	0.97	-0.01	0.04	0.00	-0.01	0.00
H_T	0.00	0.96	0.04	0.00	-0.01	0.00
H_R	0.00	0.02	0.07	0.09	0.03	0.79

Table 19: Controller Parameters of six-point control structure

Controller	CV	MV	K_c	τ_I(min)	Action
CC1	x_D(DCS)	Distillate rate	146.57	183	+
CC2	x_S(TCS)	Side-product flowrate	54.55	183	+
CC3	x_B(STC)	Reboiler duty	0.63	51	-
CC4	x_B(STC)	r_L	0.06	39	+
LC(T)	H_T	reflux rate	2	9999	+
LC(B)	H_R	Bottoms rate	2	9999	+

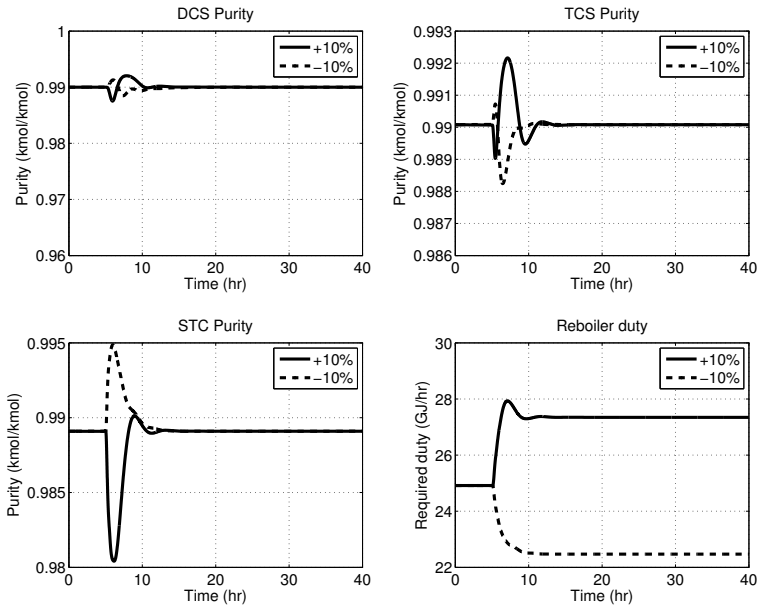

Figure 41: Results of six-point control structure

5.5 Conclusion

For the improvement of energy efficiency, DWC system was designed and their control structures were studied. Novel approach was proposed to obtain the rigorous and robust design for DWC system. As a result, designed DWC can reduce the energy consumption up to 37 % compared with classical sequential columns. The final structure is shown in Fig. 42. The total stage is 56 that is slightly lower than conventional columns of 61 (14+16+31). And also control structure of DWC system was investigated for the optimized DWC design. Three-point control structure showed a good performance, and four-point control structure could be improved a performance with faster settling time. Additionally, six-point control structure showed the most stable performance in terms of controllability and the consumed energy was the least among the case studies. Further study is needed to temperature of inferential control instead of composition controller in the future.

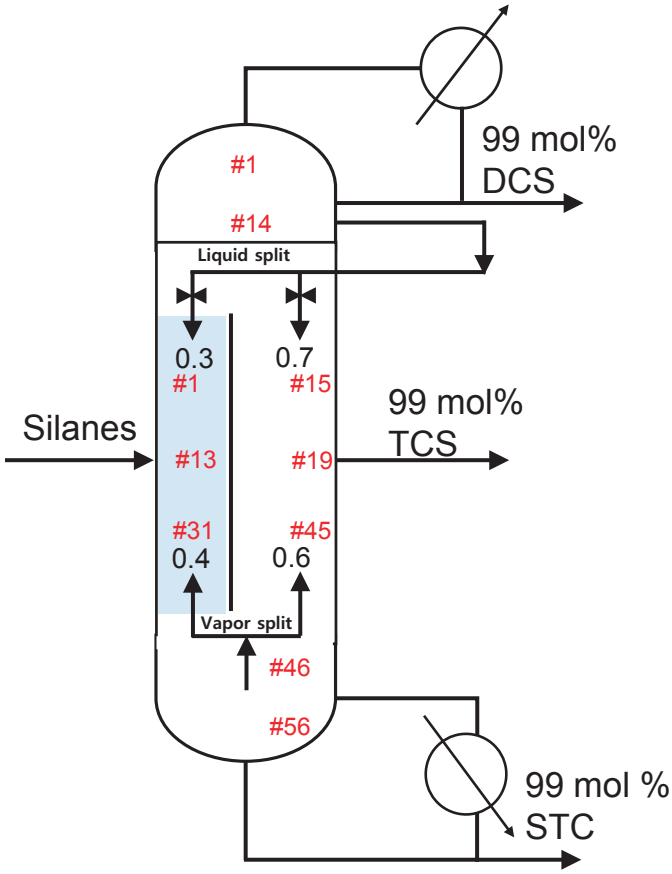

Figure 42: Final structure of DWC in silane recovery process

Chapter 6

Concluding remarks

In this thesis, a silane off-gas recovery process, which is a class of batch-continuous processes was designed with a customized CVD reactor, and a supervisory controller based on centralized MPC was developed on an industrial scale. From the simplified empirical reactor model, the OP-RP process optimization was performed, and a rigorous dynamic model was constructed to meet the annual production target. PI controllers were implemented for the regulatory layer, and the centralized MPC was established as a supervisory layer. The regulatory control did not ensure compliance with the active constraints in the cyclic steady state process, so an MPC supervisory controller was investigated.

Regulatory controllers were used to stabilize the process, and active constraints were controlled by the MPC. SVD and sensitivity analysis were used to select the temperature control tray, and the tray temperature was regulated at a constant value. In this study, as the set-points of tray temperature controllers did not changed, it was found that the centralized MPC for plant-wide scale is effective for the recovery of high-purity products. From the step response test, the relevant process input and output variables were identified within the entire process, except the tray temperature controllers. The four cases of dynamic

simulation results demonstrated that the supervisory controller satisfies all of the product constraints, and its fluctuation is much less than that using a regulatory controller only. The supervisory controller reduced the ISE about two orders of magnitude compared to PID controllers and the buffer tank also reduced the plant oscillations from the periodic disturbances. Hence, it is an option for lowering the equipment cost. Robustness of the developed control scheme was verified by unexpected abnormal situations. The results of this thesis suggest that an MPC-based supervisory controller effectively handles a process with periodic disturbances and provides simultaneous process design and control for a batch-continuous process system.

Design and control of dividing wall column was investigated in the separation of the silanes in order to maximize thermal efficiency. Four integrated columns were implemented in Aspen Dynamics^{TM}, and it was optimized. As following the proposed novel approach, it has been demonstrate that the energy consumption of DWC is expected to be reduced up to 36 % comparing the classical sequential columns. The control structure of DWC was performed, as a result, a good performance could be achieved for the thermally coupled distillation systems. Using previous demonstrations, three-point control structure and some four-point control structures were compared using an optimized four columns model of DWC. Three-point control structure was stable, and the four or six-point control structure can be reduced the settling time to minimize the energy comsumption.

Bibliography

[1] F. Jia, H. Sun, L. Koh, Global solar photovoltaic industry: an overview and national competitiveness of taiwan, Journal of Cleaner Production 126 (2016) 550–562.

[2] R. Masson, Orlandi, Global Market Outlook for Photovoltaics 2014-2018, EPIA, 2014.

[3] T. Ciszek, Photovoltaic materials and crystal growth research and development in the gigawatt era, Journal of Crystal Growth 393 (2014) 2–6.

[4] B. Ceccaroli, O. Lohne, Solar grade silicon feedstock, Handbook of Photovoltaic Science and Engineering (2003) 153–204.

[5] E. Alsema, M. de Wild-Schoten, et al., Reduction of the environmental impacts in crystalline silicon module manufacturing, in: 22nd European Photovoltaic Solar Energy Conference, WIP-Renewable Energies, 2007, pp. 829–836.

[6] Y. S. Tsuo, J. Gee, P. Menna, D. Strebkov, A. Pinov, V. Zadde, Environmentally benign silicon solar cell manufacturing, National Renewable Energy Laboratory Golden, CO, 1998.

[7] S. Chunduri, Innovations in inertia: market survey on siemens-type cvd reactors, Photon Int 4 (2013) 114–126.

[8] P. Li, T. Wang, Thermodynamic analysis of manufacturing polysilicon from sihcl 3, sicl 4 and h 2, Chinese Journal of Chemical Engineering 23 (4) (2015) 681–688.

[9] A. Ramos, A. Rodríguez, C. del Cañizo, J. Valdehita, J. Zamorano, A. Luque, Heat losses in a cvd reactor for polysilicon production: Comprehensive model and experimental validation, Journal of Crystal Growth 402 (2014) 138–146.

[10] C. Wang, T. Wang, P. Li, Z. Wang, Recycling of sicl 4 in the manufacture of granular polysilicon in a fluidized bed reactor, Chemical engineering journal 220 (2013) 81–88.

[11] A. De La Tour, M. Glachant, Y. Ménière, Innovation and international technology transfer: The case of the chinese photovoltaic industry, Energy Policy 39 (2) (2011) 761–770.

[12] F. Jia, H. Sun, L. Koh, Global solar photovoltaic industry: an overview and national competitiveness of taiwan, Journal of Cleaner Production 126 (2016) 550–562.

[13] D. Jones, D. Bhattacharyya, R. Turton, S. E. Zitney, Plant-wide control system design: Primary controlled variable selection, Computers & Chemical Engineering 71 (2014) 220–234.

[14] M. A. Schultz, D. G. Stewart, J. M. Harris, S. P. Rosenblum, M. S. Shakur, D. E. O'BRIEN, Reduce costs with dividing-wall columns, Chemical engineering progress 98 (5) (2002) 64–71.

[15] V. Sakizlis, J. D. Perkins, E. N. Pistikopoulos, Recent advances in optimization-based simultaneous process and control design, Computers & Chemical Engineering 28 (10) (2004) 2069–2086.

[16] M. Sharifzadeh, Integration of process design and control: A review, Chemical Engineering Research and Design 91 (12) (2013) 2515–2549.

[17] K. B. Sanchez-Sanchez, L. A. Ricardez-Sandoval, Simultaneous design and control under uncertainty using model predictive control, Industrial & Engineering Chemistry Research 52 (13) (2013) 4815–4833.

[18] M. Panahi, S. Skogestad, Economically efficient operation of co 2 capturing process. part ii. design of control layer, Chemical Engineering and Processing: Process Intensification 52 (2012) 112–124.

[19] H. Ryu, J. M. Lee, Model predictive control (mpc)-based supervisory control and design of off-gas recovery plant with periodic disturbances from parallel batch reactors, Industrial & Engineering Chemistry Research 55 (11) (2016) 3013–3025.

[20] L. Jianlong, C. Guanghui, P. Zhang, W. Weiwen, D. Jihai, Technical challenges and progress in fluidized bed chemical vapor deposition of polysilicon, Chinese Journal of Chemical Engineering 19 (5) (2011) 747–753.

[21] M. Hitchman, J. Kane, A. Widmer, Polysilicon growth kinetics in a low pressure chemical vapour deposition reactor, Thin Solid Films 59 (2) (1979) 231–247.

[22] J. Nishizawa, M. Saito, Mechanism of chemical vapor deposition of silicon, Journal of Crystal Growth 52 (1981) 213–218.

[23] Y. Ran, J.-B. Wang, Y.-X. Yin, Theoretical study on the sih 4- ncln (n= 0–4) reaction mechanisms for polysilicon production process, Computational and Theoretical Chemistry 1035 (2014) 60–67.

[24] L. Davis, The handbook of genetic algorithms van nostrand reingold, New York.

[25] L. Park, C. Park, C. Park, T. Lee, Application of genetic algorithms to parameter estimation of bioprocesses, Medical and biological engineering and computing 35 (1) (1997) 47–49.

[26] S.-J. Park, S. Bhargava, G. G. Chase, Fitting of kinetic parameters of no reduction by co in fibrous media using a genetic algorithm, Computers & chemical engineering 34 (4) (2010) 485–490.

[27] W. L. Luyben, Comparison of extractive distillation and pressure-swing distillation for acetone-methanol separation, Industrial & Engineering Chemistry Research 47 (8) (2008) 2696–2707.

[28] W. L. Luyben, I.-L. Chien, Design and control of distillation systems for separating azeotropes, John Wiley & Sons, 2011.

[29] W. L. Luyben, B. D. Tyreus, M. L. Luyben, Plantwide process control.

[30] N. Murthy Konda, G. Rangaiah, P. Krishnaswamy, Plantwide control of industrial processes: An integrated framework of simulation and heuristics, Industrial & engineering chemistry research 44 (22) (2005) 8300–8313.

[31] S. Skogestad, Control structure design for complete chemical plants, Computers & Chemical Engineering 28 (1) (2004) 219–234.

[32] D. Jones, D. Bhattacharyya, R. Turton, S. E. Zitney, Optimal selection of primary controlled variables for an acid gas removal unit as part of an igcc plant with co 2 capture, in: American Control Conference (ACC), 2013, IEEE, 2013, pp. 5035–5040.

[33] M. Panahi, S. Skogestad, Economically efficient operation of co 2 capturing process part i: self-optimizing procedure for selecting the best controlled variables, Chemical Engineering and Processing: Process Intensification 50 (3) (2011) 247–253.

[34] T. Larsson, M. Govatsmark, S. Skogestad, C. Yu, Control structure selection for reactor, separator, and recycle processes, Industrial & engineering chemistry research 42 (6) (2003) 1225–1234.

[35] J. H. Lee, S. Natarajan, K. S. Lee, A model-based predictive control approach to repetitive control of continuous processes with periodic operations, Journal of Process Control 11 (2) (2001) 195–207.

[36] M. Gupta, J. H. Lee, Period-robust repetitive model predictive control, Journal of Process Control 16 (6) (2006) 545–555.

[37] R. Gondhalekar, C. N. Jones, Mpc of constrained discrete-time linear periodic systems—a framework for asynchronous control: Strong feasibility, stability and optimality via periodic invariance, Automatica 47 (2) (2011) 326–333.

[38] D. Li, F. Gao, Y. Xi, Separated design of robust model predictive control for lpv systems with periodic disturbance, Journal of Process Control 24 (1) (2014) 250–260.

[39] H. Ahn, K. S. Lee, M. Kim, J. Lee, Control of a reactive batch distillation process using an iterative learning technique, Korean Journal of Chemical Engineering 31 (1) (2014) 6–11.

[40] W. L. Luyben, Distillation design and control using Aspen simulation, John Wiley & Sons, 2013.

[41] B. W. Bequette, Process control: modeling, design, and simulation, Prentice Hall Professional, 2003.

[42] W. L. Luyben, Effect of derivative algorithm and tuning selection on the pid control of dead-time processes, Industrial & engineering chemistry research 40 (16) (2001) 3605–3611.

[43] L. Wang, Model predictive control system design and implementation using MATLAB®, Springer Science & Business Media, 2009.

[44] P. Van Overschee, B. De Moor, N4sid: Subspace algorithms for the identification of combined deterministic-stochastic systems, Automatica 30 (1) (1994) 75–93.

[45] H. Ryu, J. Park, D. Lee, E. Kim, G. Ahn, S. Park, Method for manufacturing polysilicon, uS Patent App. 14/366,063 (Dec. 4 2014). URL http://www.google.com.gt/patents/US20140356535

[46] Ö. Yildirim, A. A. Kiss, E. Y. Kenig, Dividing wall columns in chemical process industry: a review on current activities, Separation and Purification Technology 80 (3) (2011) 403–417.

[47] F. Petlyuk, V. Platonov, S. DM, Thermodynamically optimal method for separating multicomponent mixtures, International Chemical Engineering 5 (3) (1965) 555.

[48] A. C. Christiansen, S. Skogestad, K. Lien, Complex distillation arrangements: Extending the petlyuk ideas, Computers & chemical engineering 21 (1997) S237–S242.

[49] G. Kaibel, Distillation-columns with longitudinal subdivision, in: Chemie Ingenieur Technik, VCH PUBLISHERS INC 303 NW 12TH AVE, DEERFIELD BEACH, FL 33442-1788, 1987, pp. 533–533.

[50] G. Parkinson, Dividing-wall columns find greater appeal, Chemical engineering progress 103 (5) (2007) 8–11.

[51] I. Dejanović, L. Matijašević, Ž. Olujić, Dividing wall column—a breakthrough towards sustainable distilling, Chemical Engineering and Processing: Process Intensification 49 (6) (2010) 559–580.

[52] A. A. Kiss, C. S. Bildea, A control perspective on process intensification in dividing-wall columns, Chemical Engineering and Processing: Process Intensification 50 (3) (2011) 281–292.

[53] H. Becker, S. Godorr, H. Kreis, J. Vaughan, Partitioned distillation columns–why, when & how, Chemical Engineering 108 (1) (2001) 68–68.

[54] G. Dünnebier, C. C. Pantelides, Optimal design of thermally coupled distillation columns, Industrial & engineering chemistry research 38 (1) (1999) 162–176.

[55] S. Wenzel, J. Rohm, et al., Design of thermally and mass-coupled distillation columns by means of total cost optimization, Chemie Ingenieur Technik 75 (5) (2003) 534–540.

[56] A. A. Kiss, J.-P. S. David, Innovative dimethyl ether synthesis in a reactive dividing-wall column, Computers & Chemical Engineering 38 (2012) 74–81.

[57] H. Ling, W. L. Luyben, New control structure for divided-wall columns, Industrial & Engineering Chemistry Research 48 (13) (2009) 6034–6049.

[58] I. J. Halvorsen, S. Skogestad, Energy efficient distillation, Journal of Natural Gas Science and Engineering 3 (4) (2011) 571–580.

[59] J. G. Segovia-Hernández, S. Hernández, A. Jiménez, Analysis of dynamic properties of alternative sequences to the petlyuk column, Computers & chemical engineering 29 (6) (2005) 1389–1399.

[60] S. Robles-Zapiain, J. G. Segovia-Hernández, A. Bonilla-Petriciolet, R. Maya-Yescas, Energy-efficient complex distillation sequences: Control properties, The Canadian Journal of Chemical Engineering 86 (2) (2008) 249–259.

[61] V. E. Tamayo-Galván, J. G. Segovia-Hernández, S. Hernández, J. Cabrera-Ruiz, J. R. Alcántara-Ávila, Controllability analysis of alternate schemes to complex column arrangements with thermal coupling for the separation of ternary mixtures, Computers & Chemical Engineering 32 (12) (2008) 3057–3066.

[62] B.-G. Rong, I. Turunen, A new method for synthesis of thermodynamically equivalent structures for petlyuk arrangements, Chemical Engineering Research and Design 84 (12) (2006) 1095–1116.

[63] F. I. Gómez-Castro, J. G. Segovia-Hernández, S. Hernandez, C. Gutiérrez-Antonio, A. Briones-Ramírez, Dividing wall distillation columns: Optimization and control properties, Chemical engineering & technology 31 (9) (2008) 1246–1260.

[64] E. Bristol, On a new measure of interaction for multivariable process control, IEEE transactions on automatic control 11 (1) (1966) 133–134.

초 록

본 논문은 폴리실리콘을 생산하는 공정에서 주기적인 외란을 포함하는 실레인 배가스를 효과적으로 회수하기 위한 공정을 설계하고, 그것을 제어하는 방법에 대하여 다루고 있다. 태양광 발전을 친환경적인 에너지원이며, 태양 전지를 만들기 위해 폴리실리콘을 재료로 사용한다. 높은 효율의 태양전지를 만들기 위해서는 고순도의 폴리실리콘이 필요하며, 고순도의 폴리실리콘을 만드는 공정은 고도의 회수공정을 수반한다. 총 28대의 기상증착 반응기를 가진 연산 1만톤 규모의 공장을 설계하였다. 유전 알고리즘을 사용하여 기상증착 반응기의 반응모델을 얻었고, 이를 이용하여 배가스로부터 수소, 염화수소, 실레인 가스를 회수하는 공정을 설계하였다. 주기적인 외란을 제거하기 위하여 비례적분 제어기를 설치하여 동적 모사를 진행하였으나, 제품 제약조건을 만족하지 못하였다. 이에 모델예측제어를 기반으로한 감시제어기를 설계하였다. 비례적분 제어기가 공정을 안정화시키고, 모델예측제어기 제품 제약조건을 제어하도록 함으로써 더 좋은 결과를 보였다. 전체 회수 공정에 대한 상세한 동적 모사 모델을 사용하여 4개의 다른 제어 구조에 대해 완충 탱크 유무에 따른 영향을 조사하였다. 분리된 실레인 배가스는 이염화실레인, 삼염화실레인, 그리고 사염화실레인 가스로 구성된다. 이 중 이염화실레인과 삼염화 실레인은 그 양을 조절하여 반응기로 재투입된다. 3가지 조성을 가진 혼합물을 저에너지로 분리하기 위해 분리벽형 증류탑을 설계하였고, 운전을 제어하는 연구를 수행하였다. 전통적인 순차 증류탑에 비해 에너지 소모를 36% 줄일 수 있었으며, 제어 구조의 연구를 통해 외란을 빠르게 제거할 수

있었다.

주요어 : 폴리실리콘, 실란 가스, 주기적인 외란, 감시제어, 모델예측제어, 분리벽형 증류탑
학번 : 2012-30254